

Polyhedra with Spherical Faces and Four-Dimensional Kleinian Groups

Kento Nakamura^a, Yoshiaki Araki^b and Kazushi Ahara^c

^aGraduate School of Advanced Mathematical Sciences, Meiji University, Tokyo, Japan;

^bJapan Tessellation Design Association;

^cSchool of Interdisciplinary Mathematical Sciences , Meiji University, Tokyo, Japan.

ABSTRACT

Quasi-Fuchsian fractals, which are announced by Ahara and Araki in 2003, are not only showing us three-dimensional fractal phenomena but also giving us opportunities for experimenting with high dimensional Kleinian groups. Nakamura and Ahara introduce an algorithm called Iterated Inversion System (IIS) in 2016 and 2017 to render these fractals, well-optimized in parallel processing. Nakamura develops and opens a system that enables us to simulate the limit sets of sphairahedra easily.

These unusual objects have many faces of studies, mathematics, computer graphics, and esthetics. In this article, we focus on observations of the mathematics side, classify the variations of sphairahedra, observe propositions, and rearrange some open problems.

KEYWORDS

visualization; fractals; Kleinian groups; circle inversion; sphere inversion

1. Introduction

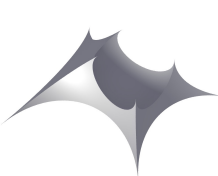
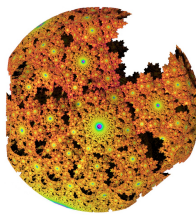
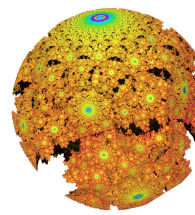


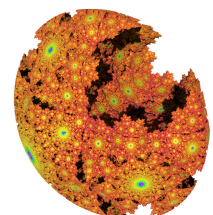
Figure 1.: Cubic



(a)



(b)



(c)

Figure 2.: Images of a quasi-sphere rendered in different view-points.

1.1. Background

The main target of this paper is a visualization of four-dimensional Kleinian groups, which is a discrete subgroup of the isometry group of that four-hyperbolic space H^4 . A four-dimensional Kleinian group G acts on S^3 , the boundary of H^4 as a Möbius transformation on S^3 .

There are few studies about a finitely generated Möbius group on S^3 , and we start at a group arising from a sphairahedron introduced by Ahara and Araki in 2003[Ahara and Araki 2003]. Sphairahedron is a coined word combining two words 'sphaira' (a prefix that means 'spherical') and 'hedron' (a suffix comes from 'polyhedron.') It looks like a polyhedron, but each face is a part of a sphere. See Figure 1. It shows a cubic sphairahedron. The polyhedral structure of the sphairahedron coincides with that of a usual cube. In the sequel, if there is no confusion, we simply call it *a cube*.

We consider a group G generated by the inversion of the six faces. An inversion is an orientation reversing isometry. Thus we consider an extended Möbius transformation group; that is, we include both orientation preserving and orientation reversion Möbius transformations and $\text{Möb}(S^3)$ denotes a group generated by all sphere-inversions in S^3 .

The group G may give a tiling by sphairahedra in S^3 . In some cases, the boundary of the tiling space converges to a three-dimensional fractal configuration. This boundary is the limit set of G . If it is homeomorphic to a two-dimensional sphere S^2 , we call it *quasi-sphere* and the group G a quasi-fuchsian group. We show an example of a quasi-sphere in Figure 2.

Ahara and Araki studied graphics and mathematics about a sphairahedron and a quasi-sphere in ICG 2002, that is, an international conference about computer graphics. The paper introduces mathematical background than the way of the rendering graphics and it shows the simplest parameter space of cubic sphairahedra and some rendered images of the limit set by POV-Ray. After that, Ahara presented a paper written in Japanese[Ahara 2003], showing the varieties of sphairahedra and dimensions of parameter space.

In the graphical aspect, in 2012, Knighty developed a script to render quasi-spheres in real-time under limited conditions¹. In 2014, Jérémie Brunet published a book of fractal paintings named "L'art fractal". One of his works in the book called "Quasi-Quasi-Grail" is based on Ahara and Araki fractal.

In 2017, a breakthrough came out. Nakamura and Ahara developed an algorithm called *Iterated Inversion System (IIS)*[Nakamura et al. 2016][Nakamura et al. 2017]. They combine IIS and Sphere tracing[Hart 1995], which is a kind of ray tracing, and their technique allows us to render quasi-spheres dramatically fast. IIS is a way to render CG related to a finitely generated group, whose generators are symmetry transformations or inversions. It determines a color on the screen pixel by pixel, thus, it get easy to parallelize and render an image fast. Rendering quasi-sphere using IIS and sphere tracing is published in Bridges[Nakamura et al. 2018], an international conference about mathematics and arts. This shows not only the way for CG but also an algorithm for mathematical art.

Note that there are many pictures of three-dimensional in this paper, but it is hard to gaze their whole appearances only on paper. We can see a fractal renderer, more pictures, and more movies based on sphairahedra in the web site² of the first author.

This paper is organaized as follows. In Section 1, we survey the history of sphairahedra and quasi-spheres. In Section 2, we prepare the definitions of a sphairahedron and its tiling group. In Section 3, we show some propositions about the parameter spaces of various kinds of sphairahedra. In Section 4, we introduce some observations.

The authors thank their colleague Shoichi Fujita in their laboratory. He provides

¹<http://www.fractalforums.com/ifs-iterated-function-systems/another-3d-kleinian/>

²<https://sphairahedron.net>

valuable comments for them to complete the calculations of the parameter spaces of cake sphairahedra.

2. Preparation

2.1. sphairahedron

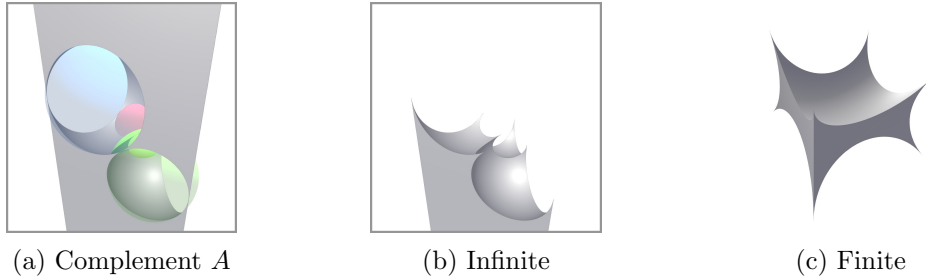


Figure 3.: sphairahedron.

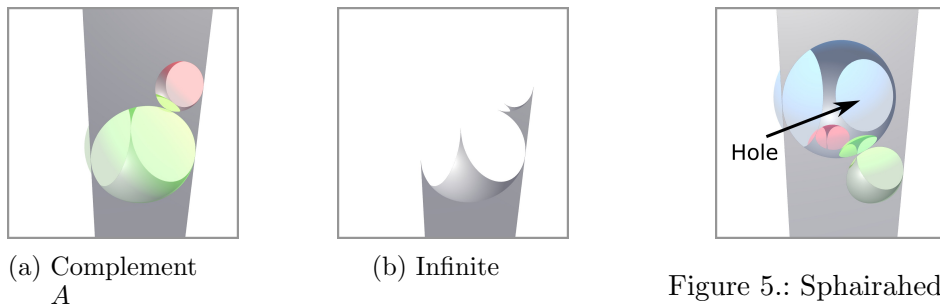


Figure 5.: Sphairahedron with hole.

Figure 4.: Semi-sphairahedron.

We describe the definition of a sphairahedron used in [Nakamura et al. 2018].

Definition 2.1. Let $S^3 = R^3 \cup \{\infty\}$ be the three-dimensional sphere and let $\overline{D_1}, \overline{D_2}, \dots, \overline{D_p}$ be three-dimensional closed balls or closed half-spaces in S^3 . We consider the complement A of the union of these balls, that is, $A = S^3 \setminus (\overline{D_1} \cup \overline{D_2} \cup \dots \cup \overline{D_p})$. If the following two conditions are satisfied, we call the component T of A a *sphairahedron*.

- (a) A consists of two connected components and all components are simply-connected.
- (b) T is a component of A , and for any i , a part of $O_i = \partial \overline{D_i}$ is a face of T .

The image in Figure 3(b)(c) is an example of a sphairahedron.

By definition, a sphairahedron has faces, edges, and vertexes. We define *ideality* and *rationality* of a sphairahedron.

Definition 2.2. (1) Let T be a sphairahedron. For each vertex, if all edges passing through the vertex are tangential to each other, we call it an *ideal* sphairahedron.

(2) Let T be a sphairahedron. For each edge, if the dihedral angle at the edge is rational (that is, the angle equals to π/n , where n is a natural number,) we call it an

rational sphairahedron.

In the sequel, we mainly consider an ideal rational sphairahedron. When one of the vertices is the infinite-point ∞ of S^3 , we call the sphairahedron *infinite sphairahedron*. One example is shown in Figure 3(b). Here, we consider a triangular prism with infinitely length and we hollow out it by three balls, and select one of the connected components as a sphairahedron. A face adjacent to the infinite vertex is a plane, the boundary of the half space. Thus the neighborhood of the infinite vertex is a prism.

When the closure of a sphairahedron does not contain the infinite point, we call it *finite sphairahedron*. See Figure 3(c).

Moreover, we can loosen the definition of an ideal rational sphairahedron, that is, we allow the case A has simply connected three or more components.

Definition 2.3. Let $\overline{D_1}, \overline{D_2}, \dots, \overline{D_p}$ be ball or half-space in S^3 . Let A be the complement of the unions of $\overline{D_i}$'s. If the following three conditions are satisfied, we call the subset T a *semi-sphairahedron*.

- (a) A has more than two connected components and all components are simply connected.
- (b) T is a component or the union of two (or more) components, and the closure $\text{Cl}(T)$ is connected.
- (c) For any i , a subset of $O_i = \partial \overline{D_i}$ is a face of T .

Figure 4(a) shows an example of a ideal rational semi-sphairahedron. We can get this shape by scooping a triangle prism out by two balls. Complement A consists of three connected components. Lower two of them are tetrahedra, and the upper one is a pentahedron. If we set T to be the unions of lower two components, then T is a semi-sphairahedron and we can regard it as a sphairahedron with a singular point. See Figure 4(b).

Remark that Ahara and Araki [Ahara and Araki 2003], and Kageyama [Kageyama 2016] did not deal with semi-sphairahedra and their rendering images.

Other than semi-sphairahedra, we have much more 'sphairahedron-like shapes' in the ideal and rational situation. See Figure 5. In this figure, we see a hole indicated by an arrow at one of the faces. This shape does not generate a sphairahedron, but we can apply the tiling method in the below section, and we have a (non-simply-connected) limit set. We have not classified these figures mathematically yet, but possibly it occurs some interesting geometry problems from here.

2.2. Limit set

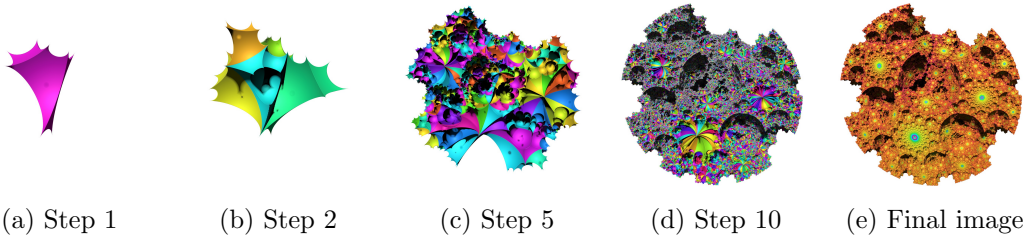


Figure 6.: Tiling of a finite cubic

Let T be a sphairahedron. Let $\overline{D_i}$ ($i = 1, 2, \dots, p$) be the closed ball of T and O_i be

the boundary sphere of $\overline{D_i}$. Suppose that a map $\varphi_i : S^3 \rightarrow S^3$ is the inversion map of O_i . φ_i is an orientation-reversing Möbius map on S^3 and let the *tiling group* $G = G(T)$ be a group generated by all φ_i 's. That is,

$$G = G(T) := \langle \varphi_1, \varphi_2, \dots, \varphi_p \rangle < \text{Mob}(S^3)$$

For a subgroup G of $\text{Mob}(S^3)$, let the *discontinuity set* $\Omega(G)$ be

$$\Omega(G) = \left\{ x \in S^3 \left| \begin{array}{l} \text{the point } x \text{ possesses a neighborhood } U(x) \text{ such that} \\ \text{that the intersection } U(x) \cap gU(x) \text{ is empty for} \\ \text{all but finite elements } g \in G \end{array} \right. \right\}.$$

The complement $\Lambda(G) := S^3 \setminus \Omega(G)$ is called the *limit set* of the group G . G is a (4 dimensional) *Kleinian group* if $\Omega(G)$ is not empty³. The limit set $\Lambda(G)$ consists either of 0 or 1 or 2 or infinitely many points. Here we consider only the case that $\Lambda(G)$ is infinite and two-dimensional. A Kleinian group G is called a *3-Kleinian group* if $\Lambda(G)$ is a round sphere. This means that G can be reduced into the Kleinian group $\text{Mob}(S^2)$ in the usual sense. A Kleinian group G is called a *quasi-fuchsian group* if $\Lambda(G)$ is homeomorphic to a closed sphere, and there exists a homeomorphism $f : S^3 \rightarrow S^3$ which conjugates G to a 3-Kleinian group. If G is a quasi-fuchsian group, the limit set $\Lambda(G)$ may be a fractal sphere, that is, a sphere embedded in S^3 with fractal structure.

Let L be the tiling generated by a tile T and a transform group G , that is, the piece set of L consists of $g(T)$ for all $g \in G$. We represent L by the pair (T, G) . The rationality condition guarantees the local consistency of tiling satisfies because of Poincaré's polyhedron theorem.

Let $|L|_k$ be the interior of the union of tiles $g(\text{Cl}(T))$ such that the word length of $g \in G$ is less than $k + 1$. That is,

$$|L|_k := \text{Int} \left(\bigcup_{(\text{length of } g) < k+1} g(\text{Cl}(T)) \right).$$

At least for a small k , $|L|_k$ is homeomorphic to a open 3-ball B^3 . For a large k there are no guarantee to be a 3-ball, though if we consider the universal covering $\widetilde{|L|_k}$ of the union of tiles, $\widetilde{|L|_k}$ is a ball for any k . There is a natural immersion $i_k : \widetilde{|L|_k} \rightarrow |L|_k \subset S^3$. The tiling $L = (T, G)$ is *embedded* in S^3 if the immersion i_k is an embedding for any k . Whether a given tiling L can be embedded in S^3 depends on the shape of the fundamental sphairahedron T and it is not trivial to show this. We call the limit $\bigcup_k |L|_k$ the *total tiling space*.

Using sphairahedron.net[Nakamura 2020], we can observe rendered images of $|L|_k$. See Figure 6. In Figure 6(a) we see the fundamental sphairahedron with six faces. $|L|_1, |L|_5, |L|_{10}$ is shown in Figure 6(b)(c)(d). In these figure, adjacent tiles have different colors. In Figure 6(d), outside tiles are so small and we see the union in gray color. These figures suggest us that $|L|_k$'s are embedded in S^3 . Figure 6(e) shows a rendering image for a large enough k . In this figure we use another algorithm(, determining a color by k on the hue circle) to render the image and we success to color the

³Usually we consider a Kleinian group as a properly discontinuous subset of the *orientation preserving* Möbius transformation group $\text{Mob}_+(S^3)$, however we weaken the condition of orientation preserving.

shape properly.

We show another example of $|L|_k$ in Figure 7. In this example the fundamental tile is an infinite sphairahedron. The resulting shape in Figure 7(e) looks like a terrain of scenic beauty.

Observation using simulator repeatedly is beneficial to find conjecture. Here we present a conjecture after observation of the simulations by sphairahedron.net [Nakamura 2020].

Conjecture 2.4. *If T is an ideal rational sphairahedron, and G is the tiling group of T , then the tiling $L = (T, G)$ is embedded in S^3 .*

Here we see the limit set of the group G . In fact it is well-known that the limit set is the closure of the accumulation point set of an orbit. Using this characteristic, we have the following.

Lemma 2.5. *If the tiling $L = (T, G)$ is embedded in S^3 , then we have*

$$\Lambda(G) = \partial \left(\bigcup_k |L|_k \right)$$

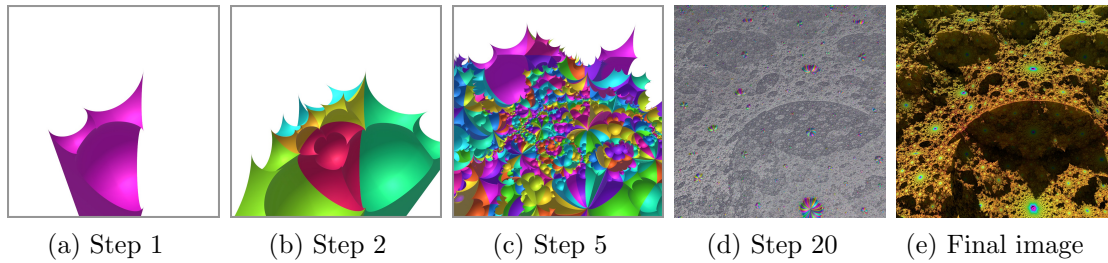


Figure 7.: Tiling of a infinite cubic sphairahedron.

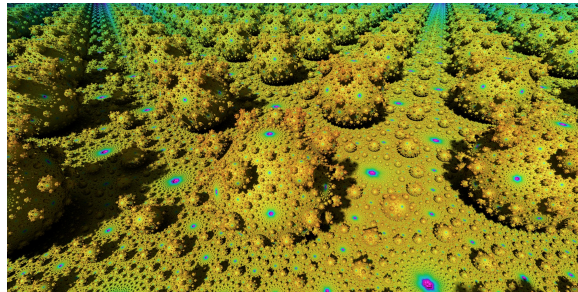


Figure 8.: Plane and infinite number of balls touching to the ground.

In the same way as above, a semi-sphairahedron can be tiled by the inversions of its faces. Though the fundamental tile may be not connected and each $|L|_k$ is not connected nor the group is not quasi-fuchsian, the closure $\text{Closure}(|L|_k)$ is connected. See an example in Figure 8. Here we see an plane and infinite number of balls touching to the ground and to each other. We call this shape *snowball fractal*. Such shape can occur lower side of the plane, that is, we see only one plane but there are infinite number of spherical pitfalls underground.

3. Parameter Spaces of Rational Ideal Sphairahedra

3.1. Classification of Sphairahedra

In this section we consider ideal rational sphairahedra of various types. In order to classify such sphairahedra, we need three steps. In the first step, we classify the polyhedral structure of a sphairahedron. See Figure 17 for a tetraheron. This example is a sphairahedron of tetrahedron type, this means that the polyhedral structure is same as that of a tetrahedron as in Figure 12. In the second step, we classify combinations of dihedral angles of edges. In tetrahedron case, there are three combinations as seen in Figure 13. Here a number n at each edge means that the dihedral angle at the edge is π/n . In the third step, we calculate the parameter space of the shape of sphairahedra. Here we assume that two sphairahedra T_1, T_2 are equivalent if there exists a (orientation preserving/reversing) Möbius transformation f on S^3 such that $f(T_1) = T_2$. In the tetrahedron case, the parameter space consists of only one point.

Ahara and Araki [Ahara and Araki 2003] determine all of combinations of dihedral angles of the cubic sphairahedra and they show one of the parameter space without a proof. Ahara [Ahara 2003] determines all of polyhedral structures of sphairahedra with 5 or 6 faces. He also shows the number of combinations of dihedral angles for each structure without a proof. Ahara and Araki [Ahara and Araki 2004] determines all of the parameter spaces for the cube case with a proof. This paper was quoted in other papers, however it is an unpublished preprint. Kageyama [Kageyama 2016] quotes the result of [Ahara and Araki 2004] in his master thesis in order to prove the existence of other variations of sphairahedra. In this chapter, we show the parameter spaces of sphairahedra with 5 or 6 faces, including current results. The proof repeats similar discussions as those in [Ahara and Araki 2004], and we enumerate the results in Appendix.

3.1.1. General lemmas

We prepare some lemmas to execute classifications.

Lemma 3.1. *Suppose that there are k edges with a vertex. Then the sum of dihedral angles of these three edges is $(k-2)\pi$. If $k=3$ then the combination of dihedral angles is one of $(\frac{\pi}{3}, \frac{\pi}{3}, \frac{\pi}{3})$, $(\frac{\pi}{2}, \frac{\pi}{4}, \frac{\pi}{4})$, and $(\frac{\pi}{2}, \frac{\pi}{3}, \frac{\pi}{6})$. If $k=4$ then the combination of dihedral angles is $(\frac{\pi}{2}, \frac{\pi}{2}, \frac{\pi}{2}, \frac{\pi}{2})$. The case $k > 4$ cannot happen.*

Proof. Let ϕ be a Möbius transformation such that it maps the vertex to the infinite-point. Then all of edges with the vertex are mapped to parallel lines, and they form a prism. If we consider a regular section of a prism, then the internal angles of the section are equal to dihedral angles, and the sum of them is $(k-1)\pi$. This completes the proof. We easily have all combinations of dihedral angles. \square

Next, we prepare some lemmas to calculate the parameter space of sphairahedra. First, we recall simple conditions to be equivalent of two sphairahedra. This lemma is clear because it is well known that these transformations are Möbius transformations.

Lemma 3.2. *Suppose that two sphairahedra T_1, T_2 satisfy that $T_2 = \varphi(T_1)$, where φ is a parallel translation or a rotation or a dilation or a plane-symmetry or a composite of these transformations. Then T_1, T_2 are equivalent.*

3.1.2. Situation 1

Next, we consider a infinite sphairahedron without loss of generality. In fact, T is a sphairahedron, and let P be one of vertices and let φ be a Möbius transformation satisfying $\varphi(P) = \infty$. Thus, $T' = \varphi(T)$ has the infinite vertex, and we may assume that one of the vertices is the infinite point.

Because of the ideality of a sphairahedron, all edges with the infinite vertex are parallel straight lines. Using rotations, we assume that these edges are parallel to the z -axis. It follows that the faces with the finite vertex are perpendicular with xy -plane.

Let A be one of finite vertices next to the infinite vertex, that is, there exists an edge e_{12} that connects A and ∞ . After applying translations, we assume that the edge e_{12} lies on the z -axis. In fact we suppose the followings as Situation 1:

$$\begin{aligned} A &= (0, 0, z_A), \\ \overline{D_1} &= \{(x, y, z) \mid 0 \leq y\} \cup \{\infty\}, \\ \overline{D_2} &= \{(x, y, z) \mid 0 \leq x \sin \theta_{12} - y \cos \theta_{12}\} \cup \{\infty\}, \\ \overline{D_3} &= \{(x - x_3)^2 + (y - y_3)^2 + (z - z_3)^2 \leq r_3^2\}, \\ O_i &= \partial(\overline{D_i}) \quad (i = 1, 2, 3,) \end{aligned}$$

where the vertex A is on the z -axis, \overline{D}_i 's are closed balls, θ_{12} is the dihedral angle of S_1 and S_2 , (x_3, y_3, z_3) is the center of the face O_3 , and r_3 is the radius of O_3 . We assume that A is the intersection of O_1, O_2, O_3 . We have the following equation including dihedral angles and x_3, y_3, z_3, r_3 .

Lemma 3.3. *In Situation (1), suppose θ_{13} is the dihedral angle of S_1 and S_3 . We have the followings.*

- (1) $z_3 = z_A$,
- (2) $r_3^2 = x_3^2 + y_3^2$,
- (3) $x_3 \cos \theta_{13} - y_3 \sin \theta_{13} = 0$.

Conversely, if \overline{D}_3 satisfies (1), (2) then the edges $O_1 \cap O_2$, $O_1 \cap O_3$, $O_2 \cap O_3$ are tangent to each other at A . If \overline{D}_3 satisfies (1), (2), and (3) then the dihedral angle of S_1 and S_3 is θ_{13} .

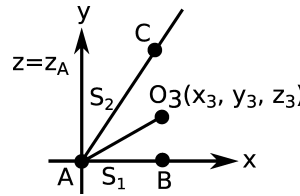


Figure 9.: Section at $a = z_A$.

Proof. Figure 9 shows the section at $z = z_A$. Let points B, C be as seen in Figure 9. By definition, $\angle BAC = \theta_{12}$. Let e_{13} be the intersection of the plane S_1 and the sphere S_3 . Then e_{13} is a circle on the xz plane and it is tangent to the z -axis at A because of the ideality. Therefore the height z_3 of the center O_3 must be the same as that A , and we have $z_3 = z_A$.

The center O_3 of S_3 lies on the section $z = z_A$ and the sphere S_3 includes the point A , hence $r_3^2 = x_3^2 + y_3^2$. Because the dihedral angle of the plane S_1 and the sphere S_3 is θ_{13} , the angle $\angle BAO_3$ is $\frac{\pi}{2} - \theta_{13}$. $x_3 \cos \theta_{13} - y_3 \sin \theta_{13} = 0$ follows immediately. \square

Remark 1. If the vertex A is of degree 3, the same observation works on the dihedral angle θ_{23} of S_2 and S_3 . In fact $\angle O_3 AC = \frac{\pi}{2} - \theta_{23}$ in Figure 9. Thus we have $\theta_{12} + \theta_{23} + \theta_{13} = \pi$ and this equation is compatible with Lemma 3.1.

After considering more general situations, we obtain the following corollary.

Corollary 3.4. *Let each O_1, O_2, O_3 be a sphere or a plane. Let $e_{ij} = O_i \cap O_j$ be a non-empty edge and let θ_{ij} be the dihedral angle of O_i and O_j . Suppose that $\theta_{12} + \theta_{23} + \theta_{13} = \pi$ and that e_{12} and e_{13} are tangent to each other at a point P . Then e_{12}, e_{13} and e_{23} are tangent at P and $O_1 \cap O_2 \cap O_3 = \{P\}$.*

3.1.3. Situation 2

We need another situation as Situation 2:

$$\begin{aligned}\overline{D_1} &= \{(x, y, z) \mid y \leq 0\} \cup \{\infty\}, \\ A &= (0, 0, 0) \\ \overline{D_2} &= \{(x, y, z) \mid (x - x_2)^2 + (y - y_2)^2 + (z - z_2)^2 < r_2^2\} \\ B &= (w, 0, z_B) \\ \overline{D_3} &= \{(x, y, z) \mid (x - x_3)^2 + (y - y_3)^2 + (z - z_3)^2 < r_3^2\} \\ O_i &= \partial(\overline{D_i}) \quad (i = 1, 2, 3,)\end{aligned}$$

where

$$\begin{aligned}z_2 &= 0, \quad r_2^2 = x_2^2 + y_2^2, \quad x_2 \cos \theta_{12} - y_2 \sin \theta_{12} = 0, \quad 0 < y_2 \\ z_3 &= z_B, \quad r_3^2 = (x_3 - w)^2 + y_3^2, \quad (x_3 - w) \cos \theta_{13} + y_3 \sin \theta_{13} = 0, \quad 0 < y_3,\end{aligned}$$

and $w(0 < w), \theta_{12}(0 < \theta_{12} \leq \frac{\pi}{2}), \theta_{13}(0 < \theta_{13} \leq \frac{\pi}{2})$ are constants. From Lemma 3.3, the dihedral angle of O_1 and O_2 (resp. O_1 and O_3) is θ_{12} (resp. θ_{13} .)

The following lemma gives a condition that two edges $O_1 \cap O_2$ and $O_1 \cap O_3$ are tangent to each other.

Lemma 3.5. *We consider a section by $y = 0$ in Situation 2 as seen in Figure 10. The left side circle is $O_1 \cap O_2$ and the right side circle is $O_1 \cap O_3$. The left circle is tangent to $x = 0$ at A and it has the center C . The right circle is tangent to $x = w$ at B and it has the center D .*

If and only if two circles are tangent to each other, the following equation holds.

$$r_2 \sin \theta_{12} + r_3 \sin \theta_{13} = \frac{w^2 + z^2}{2w}$$

Proof. The proof is very elementary, and we show it by simplified description. Let θ be $\angle CAB$. We have

$$\frac{w}{\sin \theta} = \sqrt{w^2 + z^2} = (r_2 \sin \theta_{12} + r_3 \sin \theta_{13}) \cdot (2 \sin \theta).$$

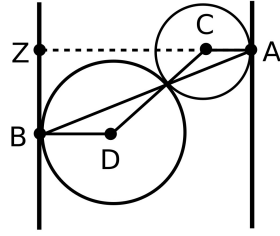


Figure 10.: Two tangent circles.

The equation $r_2 \sin \theta_{12} + r_3 \sin \theta_{13} = \frac{w^2 + z^2}{2w}$ follows immediately from these two equations. It is easy to show the converse proposition. \square

Lemma 3.6. Suppose that the condition of the above lemma is satisfies.

- (1) The dihedral angle θ_{23} of O_2 and O_3 is equal to $\pi - \theta_{12} - \theta_{13}$
- (2) The intersection edge e_{23} of O_2 and O_3 is tangent to the two circle in Figure 10 at the tangent point in the same figure.

Proof. From the cosine law, we have

$$\cos(\pi - \theta_{23}) = \frac{r_2^2 + r_3^2 - \{(x_2 - x_3)^2 + (y_2 - y_3)^2 + (z_2 - z_3)^2\}}{2r_2r_3}.$$

The coordinates of the centers of O_2 and O_3 are given by $(x_2, y_2, z_2) = (r_2 \sin \theta_{12}, r_2 \cos \theta_{12}, 0)$, and $(x_3, y_3, z_3) = (w - r_3 \sin \theta_{13}, r_3 \cos \theta_{13}, z_B)$. Using $z_B^2 + w^2 = 2w(r_2 \sin \theta_{12} + r_3 \sin \theta_{13})$, we have

$$(x_2 - x_3)^2 + (y_2 - y_3)^2 + (z_2 - z_3)^2 = r_2^2 + r_3^2 - 2r_2r_3 \cos(\theta_{12} + \theta_{13}).$$

Thus $\cos(\pi - \theta_{23}) = \cos(\theta_{12} + \theta_{13})$ and $\theta_{23} = \pi - \theta_{12} - \theta_{13}$.

(2) Let P be the tangent point in Figure 10. Applying the result of (1) to Corollary 3.4, we show that e_{23} is tangent to $O_1 \cap O_2 = e_{12}$ and $O_1 \cap O_3 = e_{13}$ at P . The proof completes. \square

3.2. Tetrahedron

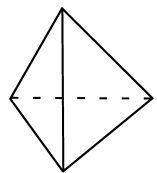


Figure 11.: Tetrahedron.

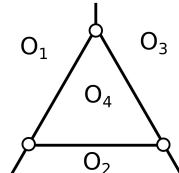
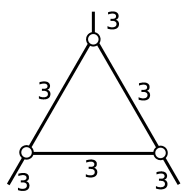
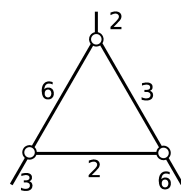


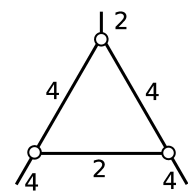
Figure 12.: Polyhedral structure.



(a) Type 1

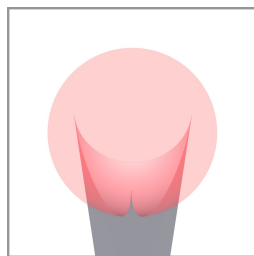


(b) Type 2

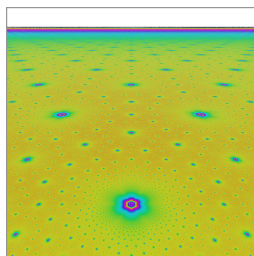


(c) Type 3

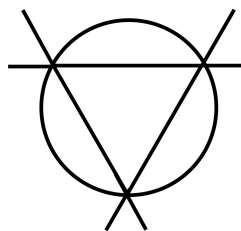
Figure 13.: Types of combinations of dihedral angles.



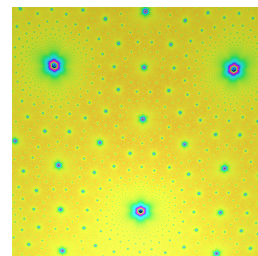
(a)



(b)

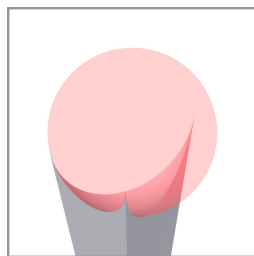


(c)

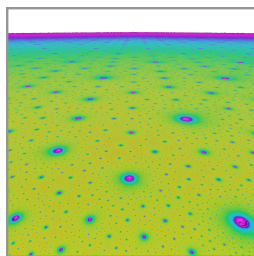


(d)

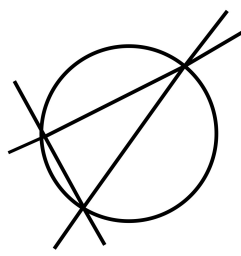
Figure 14.: A tetrahedron of type 1.



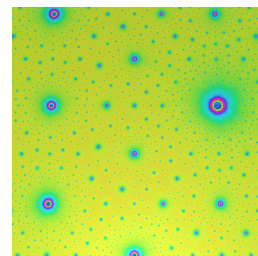
(a)



(b)

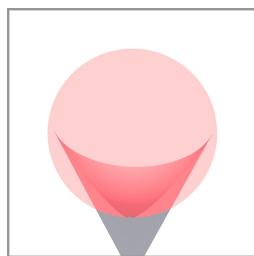


(c)

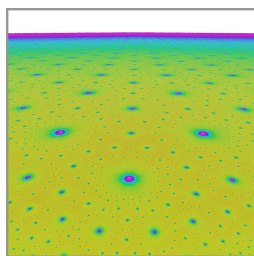


(d)

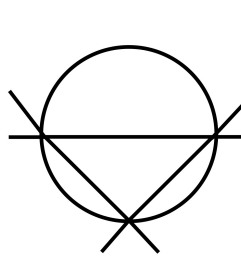
Figure 15.: A tetrahedron of type 2.



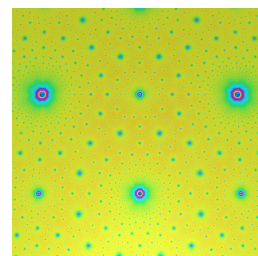
(a)



(b)



(c)

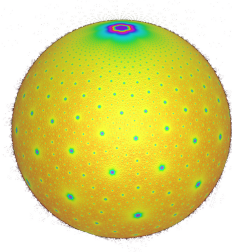


(d)

Figure 16.: A tetrahedron of type 3.



(a) Sphairahedron



(b) Limit set

Figure 17.: A finite tetrahedron of type 1.

A tetrahedron (Figure 11) has a polyhedral structure as shown in Figure 12. It is a sphairahedron with fewest faces. There are three types of combinations of dihedral angles of edges as shown in Figure 13.

Proposition 3.7. *In each type of the dihedral angles, the parameter space consists of one point.*

Proof. Suppose that one of the vertices of the sphairahedron is the infinite-point ∞ . In the type (a) case, the neighborhood of the infinite vertex is a regular triangle prism. It is because all dihedral angles equal to $\frac{\pi}{3}$. Without loss of generality, we may assume the followings.

$$\begin{aligned}\overline{D_1} &= \{(x, y, z) \mid 1 \leq x\} \cup \{\infty\} \\ \overline{D_2} &= \{(x, y, z) \mid 1 \leq -\frac{1}{2}x + \frac{\sqrt{3}}{2}y\} \cup \{\infty\} \\ \overline{D_3} &= \{(x, y, z) \mid 1 \leq -\frac{1}{2}x - \frac{\sqrt{3}}{2}y\} \cup \{\infty\} \\ \overline{D_4} &= \{(x, y, z) \mid (x - x_4)^2 + (y - y_4)^2 + (z - z_4)^2 \leq r_4^2\} \\ O_i &= \partial(\overline{D_i}) \quad (i = 1, 2, 3, 4).\end{aligned}$$

$S^3 \setminus (\overline{D_1} \cup \overline{D_2} \cup \overline{D_3})$ is the infinite triangle prism. Let a vertex P_{ijk} be $O_i \cap O_j \cap O_k$. (Generally, if the intersection of three spheres is not empty, then it consists of infinity number of points or two points or one point. In our case, the condition that the sphairahedron is ideal, the intersection is a point.) From Lemma 3.2, we may assume that $P_{124} = (1, \sqrt{3}, 0)$. Using Lemma 3.3(1), we have $z_4 = 0$ and hence $P_{234} = (-2, 0, 0)$ and $P_{134} = (1, -\sqrt{3}, 0)$. The equation $\sqrt{3}x_4 - y_4 = 0$ follows 3.3(3) and $P_{124} = (1, \sqrt{3}, 0)$. Thus we have that the center of O_4 is the origin and

$$\overline{D_4} = \{(x, y, z) \mid x^2 + y^2 + z^2 \leq 3\}.$$

This means that the parameter space of \overline{D}_i 's consists of one point. In case of another type, we show it in the same way. \square

Figures 14(a), 15(a), and 16(a) show the rendered pictures of the sphairahedra of type 1, 2, and 3 respectively.

Proposition 3.8. Assume that the tetrahedron T has the infinite vertex. In any case of dihedral angles, the limit set is the union of a plane and ∞ .

Proof. We show it in case of the type (a). Let $\overline{D_i}$'s be as in the proof of Proposition 3.7. The tetrahedron T is given by

$$T = \{(x, y, z) \mid z < 0\} \setminus (\overline{D_1} \cup \overline{D_2} \cup \overline{D_3} \cup \overline{D_4}).$$

See Figure 14(a). If we regard the lower half plane $\{(x, y, z) \mid z < 0\}$ as the hyperbolic space \mathbb{H}^3 , T is a hyperbolic ideal tetrahedron, because all edges are perpendicular to the xy -plane. For the tiling $L = (T, G)$, the boundary of the total tiling space $\cup_k |L|_k$ coincides to $\partial\mathbb{H}^3$ and the limit set is the xy -plane. \square

Indeed, the quasi-spheres are shown in Figures 14(b), 15(b), and 16(b). They are xy -plane. They have different colored patterns and it is because the combinations of the dihedral angles are different from each other. These colored patterns are shown in Figures 14(d), 15(d), and 16(d) respectively. These patterns are generated by reflections of three straight lines and one circle shown in Figures 14(c), 15(c), and 16(c) respectively. See more in Section 4.3. The tiling group G of T is 3-Kleinian. If a tetrahedron is finite, the limit set is a sphere as seen in Figure 17.

3.3. Pentahedron

3.3.1. Classification of pentahedra

There are two polyhedral structures of pentahedra. One is a quadrangular pyramid (Figure 18) and the other is a triangular prism (Figure 26.)

3.3.2. Quadrangular pyramid

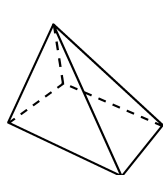


Figure 18.: Quadrangular pyramid.

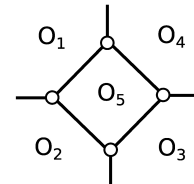


Figure 19.: Polyhedral structures.

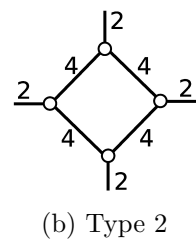
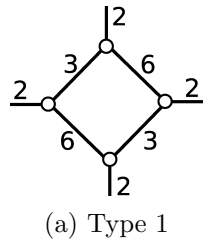


Figure 20.: Types of combinations of dihedral angles.

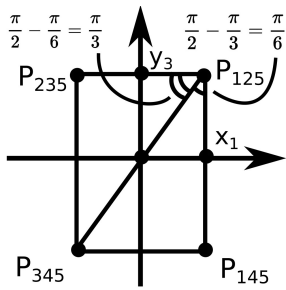


Figure 21.: Section at $z = 0$.

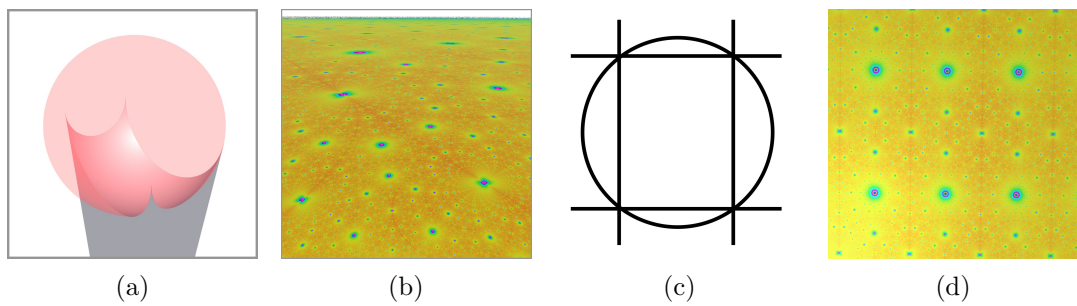


Figure 22.: A quadrangular pyramid of type 1.

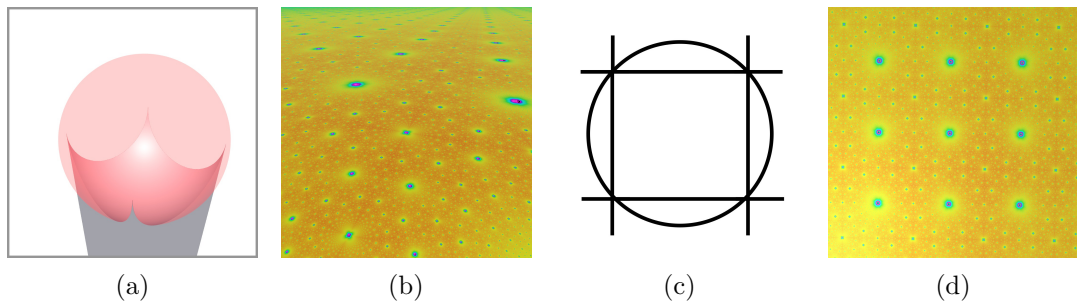


Figure 23.: A quadrangular pyramid of type 2.

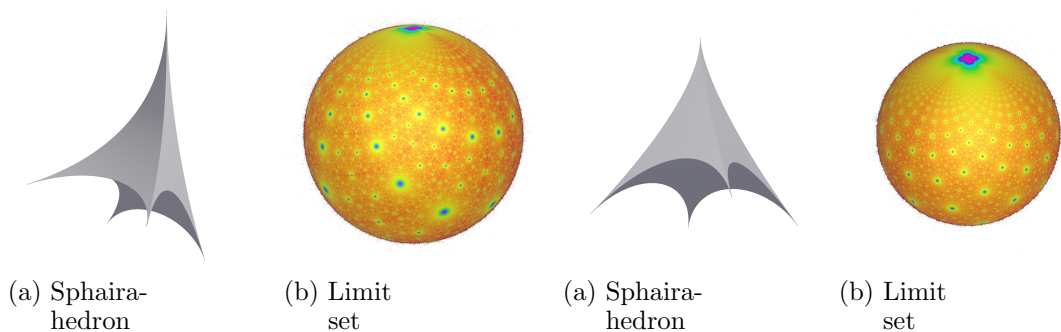


Figure 24.: Finite quadrangular pyramid type 1.

Figure 25.: Finite quadrangular pyramid type 2.

The quadrangular pyramid is a polyhedron with one basal plane and four conical faces (Figure 18.) This has a polyhedral structure as seen in Figure 19. There are two types of combinations of dihedral angle. See Figure 20. We show the parameter space as follows.

Proposition 3.9. *The parameter space of each type of dihedral angles consists of one point.*

Proof. We assume that the top-most vertex is the infinite point ∞ . Then neighborhood of ∞ is a rectangular column. Without loss of generality, we suppose the followings.

$$\begin{aligned}\overline{D_1} &= \{(x, y, z) \mid x_1 \leq x\} \cup \{\infty\} \quad (0 < x_1) \\ \overline{D_2} &= \{(x, y, z) \mid y_3 \leq y\} \cup \{\infty\} \quad (0 < y_3) \\ \overline{D_3} &= \{(x, y, z) \mid x \leq -x_1\} \cup \{\infty\} \\ \overline{D_4} &= \{(x, y, z) \mid y \leq -y_3\} \cup \{\infty\} \\ \overline{D_5} &= \{(x, y, z) \mid (x - x_5)^2 + (y - y_5)^2 + (z - z_5)^2 \leq r_5^2\} \\ O_i &= \partial \overline{D_i}\end{aligned}$$

$S^3 \setminus (\overline{D_1} \cup \overline{D_2} \cup \overline{D_3} \cup \overline{D_4})$ is a rectangular column. The vertex set is $\{P_{125}, P_{235}, P_{345}, P_{145}, \infty\}$, where $P_{ijk} = O_i \cap O_j \cap O_k$. Without loss of generality, we may suppose that P_{125} is on the xy -plane, that is, $P_{125} = (x_1, y_3, 0)$. $z_5 = 0$ follows from Lemma 3.3(1). Lemma 3.3(3) indicates that the center $(x_5, y_5, 0)$ is on the plane $\sqrt{3}(x - x_1) - (y - y_3) = 0$. See Figure 21. Because the center $(x_5, y_5, 0)$ is on the xy -plane, P_{345} must be on the same plane, that is, $P_{345} = (-x_1, -y_3, 0)$. This implies that $(x_5, y_5, 0)$ also on the plane $\sqrt{3}(x + x_1) - (y + y_3) = 0$ and hence we have $\sqrt{3}x_1 = y_3$ and $x_5 = y_5 = 0$.

Thus all of the coordinates are determined in one way except dilation and the parameter space consists of one point. In case of the type 2 of dihedral angles, we can show it in the same way. In case 2, $x_1 = y_3$ and (z_5, y_5, z_5) is the origin after all. \square

Proposition 3.10. *The limit set $\Lambda(G)$ of a sphairahedron of each type is the union of a plane and ∞ .*

Proof. The 4 vertices $P_{125}, P_{235}, P_{345}, P_{145}$ are on the xy -plane and all of the edges are perpendicular to the xy -plane. Thus the limit set is the union of the xy -plane and ∞ . See Proposition 3.8 for detail. \square

In this case, the tiling group G is 3-Kleinian after all. Figures 22(d) and 23(d) show the coloring patterns on the limit set. They are generated by the reflections of four lines and the inversion of one circle as seen in Figures 22(c) and 23(c) respectively.

3.3.3. triangular prism

A triangular prism (Figure 26) is a sphairahedron with a polyhedral structure as seen in Figure 27. There six combinations of dihedral angles as in Figures 28.

Proposition 3.11. *The parameter space of triangular prism of type 1 is an empty set. But that of semi-sphairahedra of triangular prism type 1 is an interval, one dimensional.*

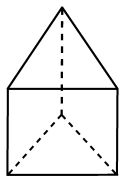


Figure 26.: Triangular prism.

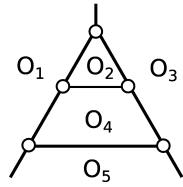
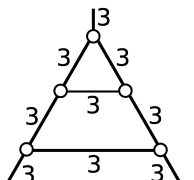
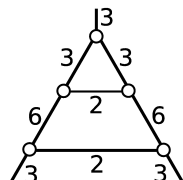


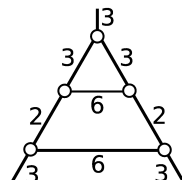
Figure 27.: Polyhedral structure.



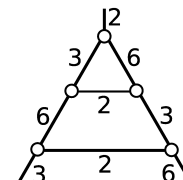
(a) Type 1



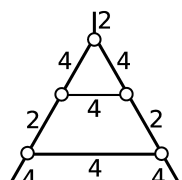
(b) Type 2



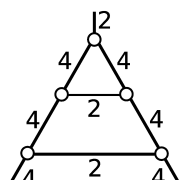
(c) Type 3



(d) Type 4



(e) Type 5



(f) Type 6

Figure 28.: Types of combinations of dihedral angles.

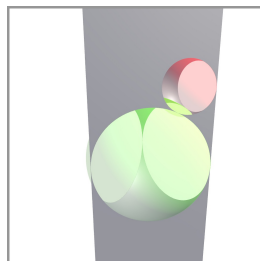
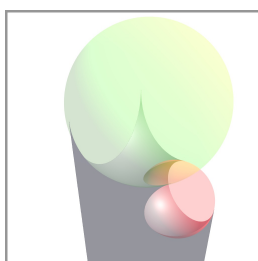
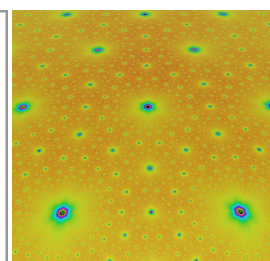


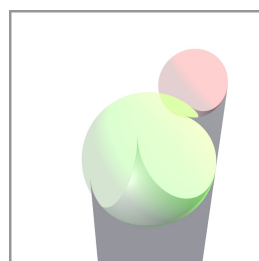
Figure 29.: Three components.



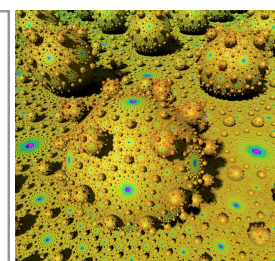
(a) Semi-sphairahedron



(b) Limit set



(a) Semi-sphairahedron



(b) Limit set

Figure 30.: Semi-sphairahedron and its limit set (1).

Figure 31.: Semi-sphairahedron and its limit set (2).

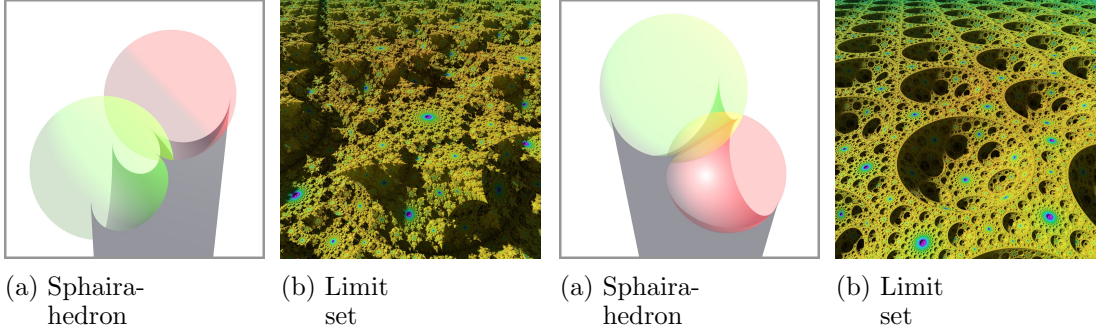


Figure 32.: Infinite triangular prism type 2 - 1. Figure 33.: Infinite triangular prism type 2 - 2.

Proof. Following Figure 27, we assume that one of the vertex is ∞ . The neighborhood of ∞ is a regular triangular column. Thus we suppose that

$$\begin{aligned}\overline{D_1} &= \{(x, y, z) \mid 1 \leq x\} \cup \{\infty\} \\ \overline{D_3} &= \{(x, y, z) \mid 1 \leq -\frac{1}{2}x - \frac{\sqrt{3}}{2}y\} \cup \{\infty\} \\ \overline{D_5} &= \{(x, y, z) \mid 1 \leq -\frac{1}{2}x + \frac{\sqrt{3}}{2}y\} \cup \{\infty\} \\ \overline{D_2} &= \{(x, y, z) \mid (x - x_2)^2 + (y - y_2)^2 + (z - z_2)^2 < r_2^2\} \\ \overline{D_4} &= \{(x, y, z) \mid (x - x_4)^2 + (y - y_4)^2 + (z - z_4)^2 < r_4^2\} \\ O_i &= \partial(\overline{D_i})\end{aligned}$$

We first determine the coordinate of $\overline{D_4}$. We may assume the height z_4 to be 0. Let P_{ijk} be $O_i \cap O_j \cap O_k$. We apply Lemma 3.3(3) at P_{145} and at P_{345} , and we obtain that $(x_4, y_4, z_4) = (0, 0, 0)$ and $r_4 = 2$. Next we consider the position of $\overline{D_2}$. The condition at P_{123} implies that (x_2, y_2, z_2) satisfies $\sqrt{3}x_2 + y_2 = 0$.

We focus on the plane $O_1 = \{(x, y, z) \mid x = 1\}$ and let r'_2 , r'_4 be the radius of the intersection circles of O_1 and O_2 , respectively (O_1 and O_4). Here we know that $r'_4 = \sqrt{3}$ is a constant. Applying Lemma 3.5 to $2r'_4 = w = 2\sqrt{3}$, we have $r'_2 = \frac{z_2^2}{2w}$, and

$$0 < \frac{z_2^2}{2w} < \frac{w}{2}.$$

This implies $-\sqrt{3} < z_2 < 0$, $0 < z_2 < \sqrt{3}$. For any z_2 satisfying these inequalities, the coordinates of all O_i 's are determined. If we consider the plane-symmetry on the xy -plane, a semi-sphericalhedron of a negative z_2 is equivalent to that of a positive z_2 .

See Figure 29. $S^3 \setminus \bigcup \overline{D_i}$ has three connected components. Thus, this $\overline{D_i}$'s do not give us a sphericalhedron but a semi-sphericalhedron. Here there are two choices of semi-sphericalhedron. One is a pentahedron (Figure 30,) and the other is the union of two tetrahedra (Figure 31.) In both cases, the tiling group G is the same group and we have one limit set of snowball fractal. \square

Proposition 3.12. *The parameter space of triangular prism of type 2 is an interval.*

Proof. In the similar way as above, we assume that one of the vertex is ∞ and the followings.

$$\begin{aligned}\overline{D_1} &= \{(x, y, z) \mid 1 \leq x\} \cup \{\infty\} \\ \overline{D_3} &= \{(x, y, z) \mid 1 \leq -\frac{1}{2}x - \frac{\sqrt{3}}{2}y\} \cup \{\infty\} \\ \overline{D_5} &= \{(x, y, z) \mid 1 \leq -\frac{1}{2}x + \frac{\sqrt{3}}{2}y\} \cup \{\infty\} \\ \overline{D_2} &= \{(x, y, z) \mid (x - x_2)^2 + (y - y_2)^2 + (z - z_2)^2 < r_2^2\} \\ \overline{D_4} &= \{(x, y, z) \mid (x - x_4)^2 + (y - y_4)^2 + z^2 < r_4^2\} \\ O_i &= \partial(\overline{D_i})\end{aligned}$$

Immediately we have $(x_4, y_4) = (-\frac{1}{2}, \frac{\sqrt{3}}{2})$ and $r_4 = \sqrt{3}$. We consider the face O_1 and let r'_2, r'_4 be the radius of the intersection circles of O_1 and O_2 , respectively O_1 and O_4 .) Here $r'_4 = \frac{\sqrt{3}}{2}$. Using Lemma 3.5, we have $r'_2 = \frac{6+z_2^2}{4\sqrt{3}}$. Thus an inequality

$$\frac{6+z_2^2}{4\sqrt{3}} < \sqrt{3} (= \frac{w}{2})$$

follows from the condition of O_2 and this implies $-\sqrt{6} < z_2 < \sqrt{6}$. For any z_2 contained in this interval determines a sphairahedron. Thus the parameter space of sphairahedra of type 2 is an open interval. See Figures 32, 33. These are typical terrains of triangular prisms. A positive z_2 gives us a shape as seen in Figure 32, and a negative z_2 for Figure 33. \square

In the similar way, we have the following proposition.

Proposition 3.13. *The parameter spaces of sphairahedra of from type 3 to type 6 are empty sets. But that of semi-sphairahedra of each type is an open interval, one dimensional.*

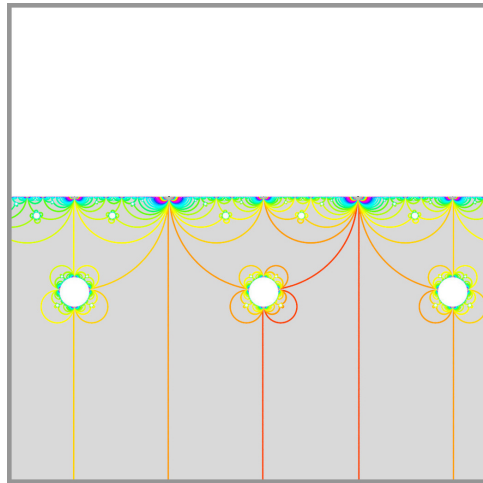


Figure 34.: Slice image of the limit set of a semi-sphairahedron of type 3.

Among type 3 and type 5, we have another shape of the limit set. For example, the limit set of a semi-sphairahedron of type 3 is a infinite number of disjoint spheres. Figure 34 shows rendered images of a semi-sphairahedron and a section of the tiling configuration. The white circles are cavities and the limit set, the boundary, is the infinite union of spheres.

3.4. Hexahedron (1), cube

3.4.1. Classification of hexahedra

There are 7 polyhedral structures of hexahedra. They are:

- (a) cube (Figure 35),
- (b) cake 1 (Figure 43),
- (c) cake 2 (Figure 46),
- (d) cake 3 (Figure 55),
- (e) cake 4 (Figure 62),
- (f) pentagonal pyramid (Figure 63),
- (g) triangular dipyramid (Figure 64).

In this list, the cube and the cake1 have lots of varieties. In this subsection, we introduce the cube. Ahara and Araki [Ahara and Araki 2004] show the classification of the cubes precisely. This preprint is sometimes quoted but is not published, thus we check the proof of the theorem again and list the result up.

3.4.2. Classification of cubes

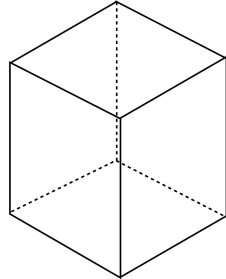


Figure 35.: Cube.

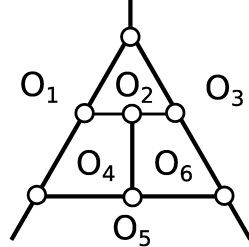


Figure 36.: Polyhedral structure.

A cube (Figure 35) is a sphairahedron with a polyhedral structure as seen in Figure 36. There are 11 combinations of dihedral angles as seen in Figure 37.

3.4.3. Parameter spaces of cubes

The parameter space of each type of the cube is as followings.

Proposition 3.14. (1) For types 1, 2, 3, 4, 5, 8, and 9, the parameter spaces of cubes are two dimensional. The boundary of each parameter space consists of straight lines or hyperbolas.

(2) For types 6, 7, 10, 11, the parameter space is empty.

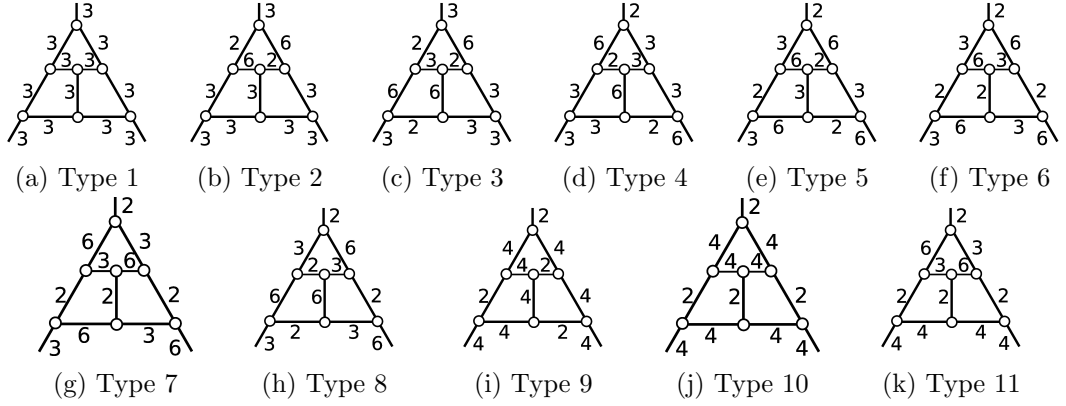


Figure 37.: Types of combinations of dihedral angles.

3.4.4. Parameter spaces of cubes of type 1

We refer the precise proof for type 1 from [Ahara and Araki 2004].

The vertex set is $\{P_{123}, P_{145}, P_{356}, P_{124}, P_{456}, P_{236}, P_{246}, P_{135}\}$, where $P_{ijk} = O_i \cap O_j \cap O_k$. Without loss of generality, we assume that P_{135} is ∞ .

Suppose \overline{D}_i 's are as follows:

$$\begin{aligned}\overline{D}_1 &= \{(x, y, z) \mid \frac{1}{2} \leq x\} \cup \{\infty\} \\ \overline{D}_3 &= \{(x, y, z) \mid \frac{1}{2} \leq -\frac{1}{2}x - \frac{\sqrt{3}}{2}y\} \cup \{\infty\} \\ \overline{D}_5 &= \{(x, y, z) \mid \frac{1}{2} \leq -\frac{1}{2}x + \frac{\sqrt{3}}{2}y\} \cup \{\infty\} \\ \overline{D}_2 &= \{(x, y, z) \mid (x - x_2)^2 + (y - y_2)^2 + z^2 < r_2^2\} \\ \overline{D}_4 &= \{(x, y, z) \mid (x - x_4)^2 + (y - y_4)^2 + (z - z_4)^2 < r_4^2\} \\ \overline{D}_6 &= \{(x, y, z) \mid (x - x_6)^2 + (y - y_6)^2 + (z - z_6)^2 < r_6^2\} \\ O_i &= \partial(\overline{D}_i)\end{aligned}$$

Step 1: In this step, we get conditions for these \overline{D}_i 's to establish a cube of type 1. Let θ_{ij} be the dihedral angle of O_i and O_j , and let w_i be the width of the face O_i ($i = 1, 3, 5$.) In case of type 1, $\theta_{ij} = \frac{\pi}{3}$ for any existing θ_{ij} , and $w_i = 2\sqrt{3}$. The three equations bellow follow immediately from Lemma 3.5.

$$\begin{aligned}r_2 \sin \theta_{12} + r_4 \sin \theta_{14} &= \frac{w_1^2 + z_4^2}{2w_1} \\ r_2 \sin \theta_{23} + r_6 \sin \theta_{36} &= \frac{w_3^2 + z_6^2}{2w_3} \\ r_4 \sin \theta_{45} + r_6 \sin \theta_{56} &= \frac{w_5^2 + (z_4 - z_6)^2}{2w_5}\end{aligned}\tag{*}$$

Remark that these equations (*) hold for other types of the dihedral angles. Solving

the above system of equations, we have:

$$\begin{aligned} r_2 &= \frac{2z_4z_6 + 3}{6} \\ r_4 &= \frac{2z_4(z_4 - z_6) + 3}{6} \\ r_6 &= \frac{2z_6(z_6 - z_4) + 3}{6}. \end{aligned} \tag{**}$$

Here, notice that if z_4 and z_6 are given, we get the value of r_2 , r_4 , and r_6 . Here we have some conditions to establish a cube. One is r_2 , r_4 , and r_6 are positive. Secondly, $O_2 \cap O_5 = \emptyset$, $O_4 \cap O_3 = \emptyset$, and $O_6 \cap O_1 = \emptyset$. Thus, we obtain:

$$0 < r_2 < \frac{3}{4}, \quad 0 < r_6 < \frac{3}{4}, \quad 0 < r_6 < \frac{3}{4},$$

and hence

$$\begin{aligned} -\frac{3}{2} < z_4z_6 < \frac{3}{4}, \quad -\frac{3}{2} < z_4(z_4 - z_6) < \frac{3}{4}, \quad -\frac{3}{2} < z_6(z_6 - z_4) < \frac{3}{4} \\ \Leftrightarrow z_4z_6 &< \frac{3}{4}, \quad z_4(z_4 - z_6) < \frac{3}{4}, \quad z_6(z_6 - z_4) < \frac{3}{4} \end{aligned} \tag{*}$$

See Figure 39. This is the area representing (*).

Step 2: In this step, we first determine the values (z_4, z_6) satisfying (*) and show that this gives a cube (= cubic sphairahedron). Indeed, suppose that the centers and radii of O_2, O_4, O_6 are given by followings.

The center and the radius of O_2 :

$$\begin{aligned} (x_2, y_2, z_2) &= \left(\frac{1}{2}(1 - r_2), -\frac{\sqrt{3}}{2}(1 - r_2), 0 \right), \\ r_2 &= \frac{2z_4z_6 + 3}{6}. \end{aligned}$$

The center and the radius of O_4 :

$$\begin{aligned} (x_4, y_4, z_4) &= \left(\frac{1}{2}(1 - r_4), \frac{\sqrt{3}}{2}(1 - r_4), z_4 \right), \\ r_4 &= \frac{2z_4(z_4 - z_6) + 3}{6}. \end{aligned}$$

The center and the radius of O_6 :

$$\begin{aligned} (x_6, y_6, z_6) &= (r_6 - 1, 0, z_6), \\ r_6 &= \frac{2z_6(z_6 - z_4) + 3}{6}. \end{aligned}$$

It is enough for us to check the following lemma.

Lemma 3.15. *Let the edge e_{ij} be $O_i \cap O_j$.*

(1) The edges e_{12}, e_{13}, e_{23} are tangent to each other at a point. The edges e_{14}, e_{15}, e_{45} are tangent to each other at a point. The edges e_{35}, e_{36}, e_{56} are tangent to each other at a point.

The dihedral angle at e_{12} is $\theta_{12} = \frac{\pi}{3}$. The dihedral angle at e_{14} is $\theta_{14} = \frac{\pi}{3}$. The dihedral angle at e_{23} is $\theta_{23} = \frac{\pi}{3}$. The dihedral angle at e_{36} is $\theta_{36} = \frac{\pi}{3}$. The dihedral angle at e_{45} is $\theta_{45} = \frac{\pi}{3}$. The dihedral angle at e_{56} is $\theta_{56} = \frac{\pi}{3}$.

(2) The dihedral angle at e_{24} is $\theta_{24} = \frac{\pi}{3}$. The edges e_{12}, e_{14}, e_{24} are tangent to each other at a point. The dihedral angle at e_{26} is $\theta_{26} = \frac{\pi}{3}$. The edges e_{23}, e_{26}, e_{36} are tangent to each other at a point. The dihedral angle at e_{46} is $\theta_{46} = \frac{\pi}{3}$. The edges e_{45}, e_{46}, e_{56} are tangent to each other at a point.

(3) The edges e_{24}, e_{26}, e_{46} are tangent to each other at a point.

Proof. (1) Using Lemma 3.3, we show these straightforward.

(2) Applying Lemma 3.6 to the equations (*), we show these straight forward.

(3) This is non-trivial. Let α be a plane containing three centers of the spheres O_2, O_4, O_6 . (Here O_2, O_4, O_6 denote their center.) Let C_2, C_4, C_6 be three circles on α such that C_i is the intersection of the sphere O_i and the plane α . ($i = 2, 4, 6$.) Let R be the radical point of C_2, C_4, C_6 . There are three cases here. (i) R is inside if C_2, C_4, C_6 . (ii) R is outside C_2, C_4, C_6 . (iii) R is on C_2, C_4, C_6 . (See Figure 38.)

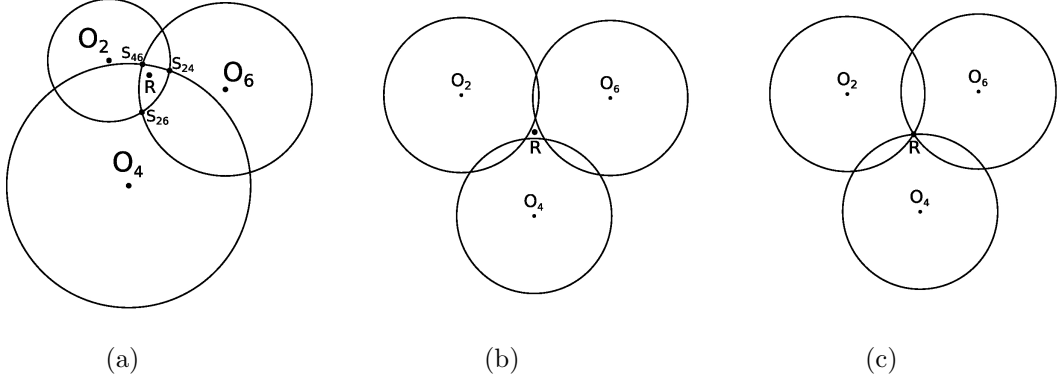


Figure 38.: Condition of circles.

In the case (i), let three points S_{24}, S_{46}, S_{26} be as in Figure 38 (a). Here we have $\angle O_2 S_{24} O_4 = \pi - \theta_{24}$, because their dihedral angle of O_2 and O_4 is θ_{24} . In the same way, $\angle O_4 S_{46} O_6 = \pi - \theta_{46}$ and $\angle O_2 S_{26} O_6 = \pi - \theta_{26}$ hold. Hence

$$\angle O_2 S_{24} O_4 + \angle O_4 S_{46} O_6 + \angle O_2 S_{26} O_6 = 3\pi - \theta_{24} - \theta_{46} - \theta_{26} = 2\pi.$$

On the other hand, from Figure 38 (a)

$$\angle O_2 S_{24} O_4 < \angle O_2 R O_4, \quad \angle O_2 S_{26} O_6 < \angle O_2 R O_6, \quad \angle O_4 S_{46} O_6 < \angle O_4 R O_6$$

and

$$\angle O_2 R O_4 + \angle O_4 R O_6 + \angle O_2 R O_6 = 2\pi$$

This is a contradiction. Thus this case cannot occur. In the same way, the case (ii)

cannot happen. It follows that the radical point R is on the intersection of three circles C_2, C_4, C_6 . This means that R is the unique intersection of 3 spheres O_2, O_4, O_6 and $R = P_{246}$. \square

Replacing (z_4, z_6) with (z_A, z_B) , we show the deciding parameter space of cubes of type 1 as seen in Figure 40. Here, because of symmetry of combinations of dihedral angles, we may assume that $z_B \geq 2z_A$.

There are 6 cases of the order of $0, z_A, z_B$ and for each case, we can replace (z_A, z_B) with another parameters. In fact

$$\begin{aligned} z_A < z_B < 0 &\Rightarrow (z_A, z_B) \mapsto (z_B - z_A, -z_A). \\ z_A < 0 < z_B &\Rightarrow (z_A, z_B) \mapsto (-z_A, z_B - z_A). \\ z_B < z_A < 0 &\Rightarrow (z_A, z_B) \mapsto (z_A - z_B, -z_B). \\ z_B < 0 < z_A &\Rightarrow (z_A, z_B) \mapsto (-z_B, z_A - z_B). \\ 0 < z_B < z_A &\Rightarrow (z_A, z_B) \mapsto (z_B, z_A). \\ 0 < z_A \leq z_B < 2z_A &\Rightarrow (z_A, z_B) \mapsto (z_B - z_A, z_B). \end{aligned}$$

In this way, the correct parameter space is as seen in Figure 40.

Here if (z_A, z_B) is on the Hyperbola $z_B^2 - z_A z_B = 3/4$, then the face O_2 touches O_5 . Moreover if (z_A, z_B) is on the point $A(\sqrt{6}/4, \sqrt{6}/2)$ then O_2 touches O_5 and O_3 touches O_4 . These case a singular shape of a cube of type 1

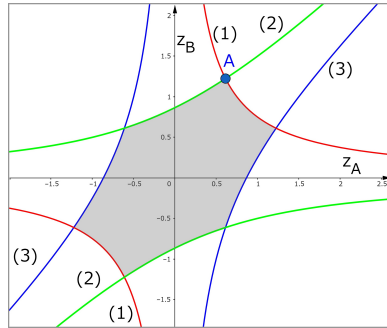


Figure 39.: Parameter space without limitation.

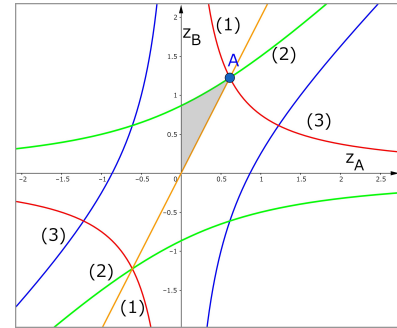


Figure 40.: Parameter space limited by symmetry.

$$\begin{aligned} (1) z_A z_B &= 3/4 \\ (2) z_B^2 - z_A z_B &= 3/4 \\ (3) z_A^2 - z_A z_B &= 3/4 \end{aligned}$$

3.4.5. Parameter space of cubes of other types

In the same way of calculations, we have similar results in case of types 2, 3, 4, 5, 8, and 9. We show the parameter spaces in each case. The figures will be shown in Appendix.

Type 2: (Figure 74)

$$\begin{cases} 0 < -2\sqrt{3}z_A z_B + 54 - 30\sqrt{3} \\ 0 < -3z_A^2 + 4z_A z_B + 15/4 \\ 0 < 2z_A z_B - 3z_B^2 + 3/4 \end{cases}$$

Type 3: (Figure 75)

$$\begin{cases} 0 < -\sqrt{3}z_A^2 - 2\sqrt{3}z_A z_B + 90 - 51\sqrt{3} \\ 0 < -3\sqrt{3}z_A^2 + 4\sqrt{3}z_A z_B + 90 - 48\sqrt{3} \\ 0 < z_A^2 + 2z_A z_B - 5z_B^2 + 9/4 \end{cases}$$

Type 4: (Figure 76)

$$\begin{cases} 0 < -3z_A^2 - 6z_A z_B - z_B^2 - 60 + 36\sqrt{3} \\ 0 < -15z_A^2 + 6z_A z_B + z_B^2 - 120 + 72\sqrt{3} \\ 0 < 3z_A^2 + 6z_A z_B - 5z_B^2 - 120 + 72\sqrt{3} \end{cases}$$

Type 5: (Figure 77)

$$\begin{cases} 0 < -6z_A z_B - z_B^2 + 9/4 \\ 0 > 7z_A^2 - 6z_A z_B - z_B^2 - 3 \\ 0 < z_A z_B - z_B^2 - 24 + 14\sqrt{3} \end{cases}$$

Type 8: (Figure 78)

$$\begin{cases} 0 < -3z_A^2 - 2z_A z_B + 3/4 \\ 0 < -3z_A^2 + 3z_A z_B + 2 \\ 0 < 3z_A^2 + 2z_A z_B - 5z_B^2 + 3 \end{cases}$$

Type 9: (Figure 79)

$$\begin{cases} 0 < -2z_A z_B - z_B^2 + 1 \\ 0 < -3z_A^2 + 2z_A z_B + z_B^2 + 2 \\ 0 < z_A z_B - z_B^2 - 8 + 6\sqrt{2} \end{cases}$$

In case of type 6, 7, 10, and 11, there is no solution of parameters to be a cube. We can obtain systems of inequalities but there are no intersection of these systems. In fact, in case of type 6,

$$\begin{cases} 0 < \frac{z_A z_B}{\sqrt{3}} < \frac{\sqrt{3}}{4} \\ 0 < \frac{1 + z_B^2 - z_A z_B}{2} < \frac{1}{2} \\ 0 < \frac{3 + z_C^2 - z_A z_B}{2\sqrt{3}} < \frac{\sqrt{3}}{2}. \end{cases}$$

In case of type 7,

$$\begin{cases} 0 & < \frac{z_A z_B}{2} < \frac{\sqrt{3}}{2 + \sqrt{3}} \\ 0 & < \frac{2 + 2z_B^2 - z_A z_B}{4} < \frac{1}{2} \\ 0 & < \frac{\sqrt{3}(6 + 2z_C^2 - 3z_A z_B)}{12} < \frac{\sqrt{3}}{2} \end{cases}$$

In case of type 10,

$$\begin{cases} 0 & < \frac{z_A z_B}{2} < \frac{1}{2} \\ 0 & < \frac{\sqrt{2}(2 + z_B^2 - z_A z_B)}{4} < \frac{\sqrt{2}}{2} \\ 0 & < \frac{\sqrt{2}(2 + z_C^2 - z_A z_B)}{4} < \frac{\sqrt{2}}{2} \end{cases}$$

In case of type 11,

$$\begin{cases} 0 & < \frac{2z_A z_B}{\sqrt{6} + \sqrt{2}} < \frac{1}{\cos(\pi/12 + 1)} \\ 0 & < \frac{\sqrt{2}(2(1 + \sqrt{3}) + (1 + \sqrt{3})z_B^2 - 2z_A z_B)}{2(\sqrt{6} + \sqrt{2})} < \frac{\sqrt{2}}{2} \\ 0 & < \frac{\sqrt{2}(2(1 + \sqrt{3}) + (1 + \sqrt{3})z_C^2 - 2\sqrt{3}z_A z_B)}{2(\sqrt{6} + \sqrt{2})} < \frac{\sqrt{2}}{2} \end{cases}$$

In these cases, there is no answer for (z_A, z_B) .

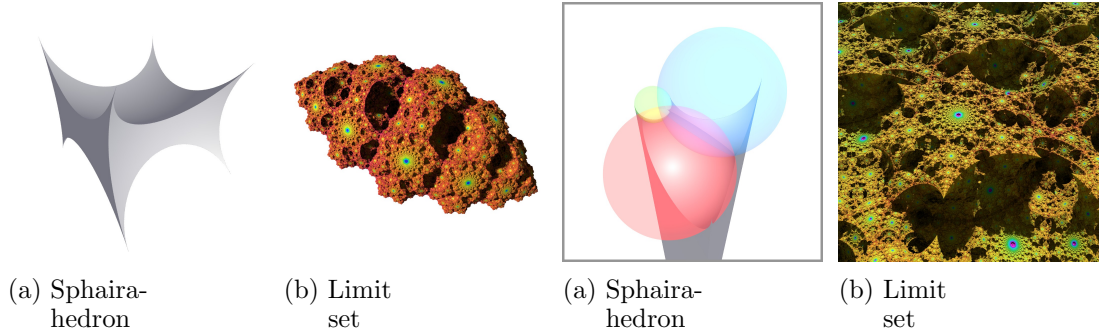


Figure 41.: Finite cubic sphairahedron and Figure 42.: Infinite cubic sphairahedron and limit set.

Figures 41, 42 give rendered images of cubes and their limit set. To render these images, the first author uses IIS algorithm [Nakamura et al. 2018].

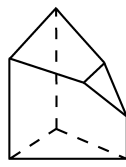


Figure 43.: Cake #1.

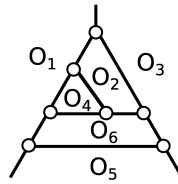


Figure 44.: Polyhedral structure.

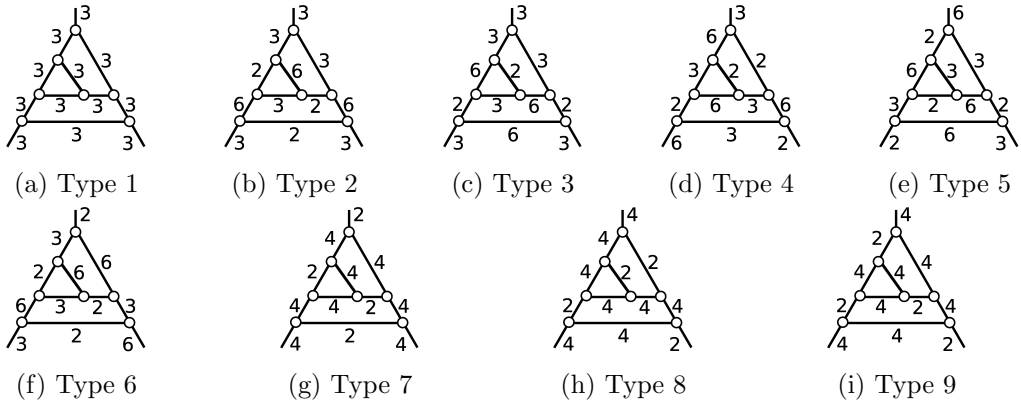


Figure 45.: Combinations of dihedral angles of cake #1.

3.5. Hexahedron (2), others

3.5.1. Cake #1

Some of hexahedra do not have their unique name, and we give names to them. We name Figures 43, 46, 55, and 62 *cakes* with a serial number from 1 to 4. In this subsection we introduce a cake #1. Its polyhedral structure is as seen in Figure 44. (It looks like a sponge cake.) There are 9 types of combinations of dihedral angles. See Figures from 45(a) to 45(i).

Investigation of the parameter space of cakes #1 has not completed. For long time the authors studied this object, but it is still open. We may assume that the three half-spaces $\overline{D_1}, \overline{D_3}, \overline{D_5}$ form a (vertical) triangular prism. and we may fix the height of $\overline{D_6}$. If we choose heights of $\overline{D_2}$ and $\overline{D_4}$, we may determine a cake #1 sphairahderon. Thus the parameter space might be two dimensional if it exists.

3.5.2. Cake #2

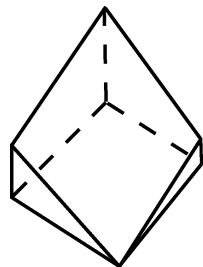


Figure 46.: Cake #2.

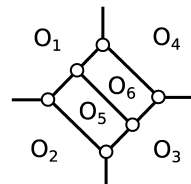
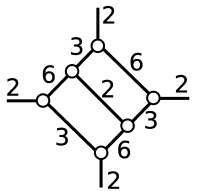
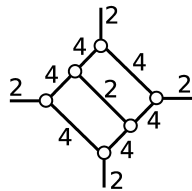


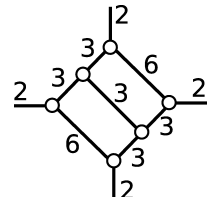
Figure 47.: Polyhedral structure.



(a) Type 1



(b) Type 2

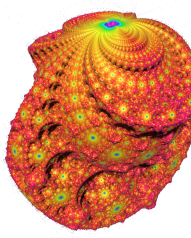


(c) Type 3

Figure 48.: Combinations of dihedral angles of cake #2.

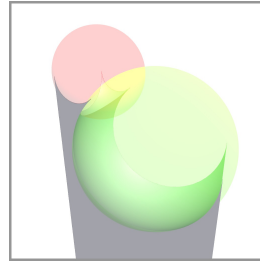


(a) Sphairahedron

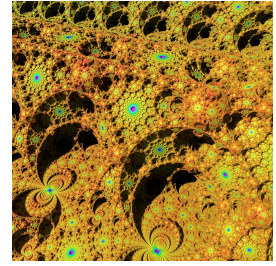


(b) Limit set

Figure 49.: Finite cake #2 type 1.

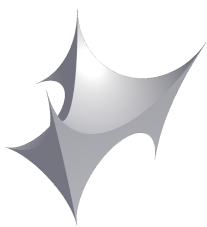


(a) Sphairahedron

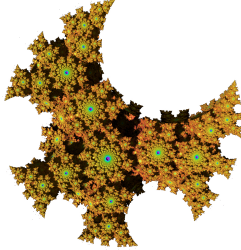


(b) Limit set

Figure 50.: Infinite cake #2 type 1.

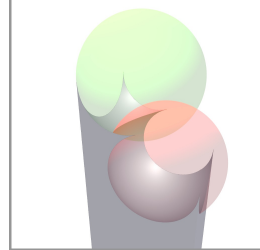


(a) Sphairahedron

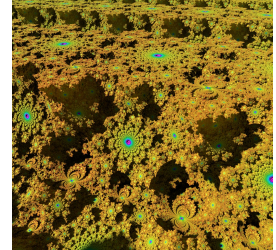


(b) Limit set

Figure 51.: Finite cake #2 type 2.



(a) Sphairahedron



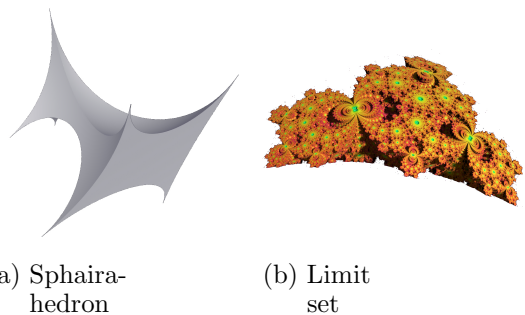
(b) Limit set

Figure 52.: Finite cake #2 type 2.

The hexahedral cake #2 is as seen in Figure 46. (It looks like a short bread.) Figure 47 shows its polyhedral structure. There are three combinations of dihedral angles. See Figure 48. The parameter space of each type is one dimensional. We show their precise data in Appendix.

3.5.3. Cake #3

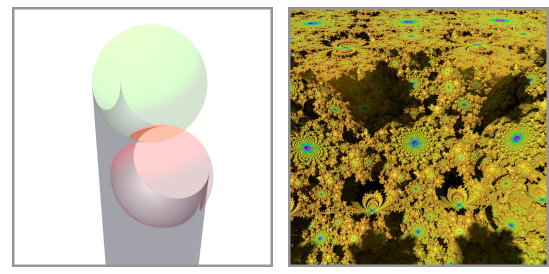
The hexahedral cake #3 is as seen in Figure 55. (It looks like a chiffon cake.) Figure 56 shows its polyhedral structure. There are three combinations of dihedral angles. See Figure 57. There is no cake #3 sphairahedron. The reason is very similar as that of a triangular prism. The parameter space of semi-sphairahedra are one dimensional for each. We show their precise data in Appendix.



(a) Sphaira-hedron

(b) Limit set

Figure 53.: Finite cake #2 type 3.



(a) Sphaira-hedron

(b) Limit set

Figure 54.: Infinite cake #2 type 3.

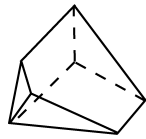


Figure 55.: Cake #3.

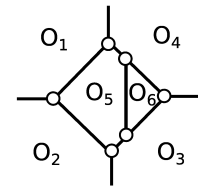
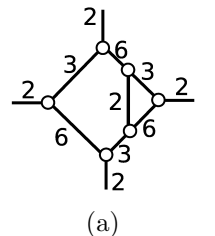
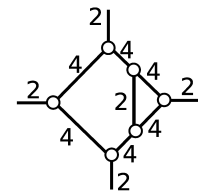


Figure 56.: Polyhedral structure.

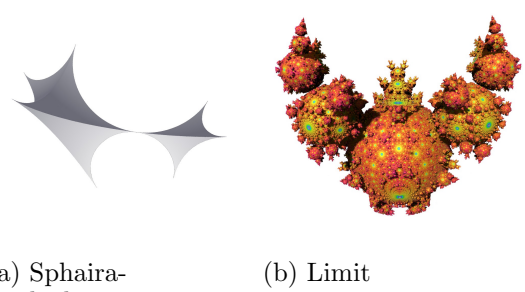


(a)



(b)

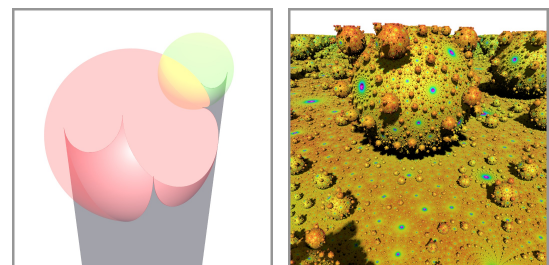
Figure 57.: Combinations of dihedral angles of cake #3.



(a) Sphaira-hedron

(b) Limit set

Figure 58.: Finite hexahedral cake #3 type 1.



(a) Sphaira-hedron

(b) Limit set

Figure 59.: Infinite hexahedral cake #3 type 1.

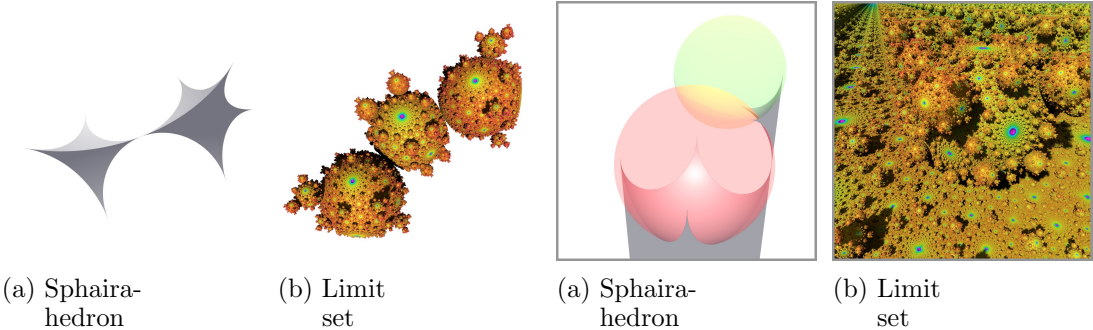


Figure 60.: Finite hexahedral cake #3 type 2.

Figure 61.: Infinite hexahedral cake #3 type 2.

3.5.4. Other hexahedra

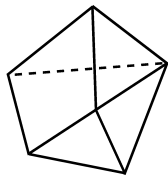


Figure 62.: Hexahedral cake #4.

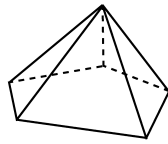


Figure 63.: Pentagonal pyramid.

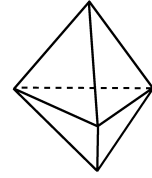


Figure 64.: Triangular dipyramid.

The remaining hexahedra are a cake #4 (Figure 62,) a pentagonal pyramid (Figure 63,) and a triangular dipyramid (64.) They has no combination of dihedral angles.

3.6. Polyhedra whose number of the faces is seven and more

It seems challenging to compute rational ideal sphairahedra based on heptahedron or polyhedra with more faces. Indeed, counting up the combinations of dihedral angles is an open problem. In this subsection, we show the condition to be a rational ideal sphairahedron and find some examples.

From Lemma 3.1, we know that the degree of each vertex must be equal to or less than 4. Moreover, if a polyhedron satisfies this condition, we have to consider a combination of dihedral angles.

We can find three simple examples soon. One is a regular dodecahedron. All of the faces are pentagons, and this is trivalent, that is, the degree of each vertex is 3. Thus if we assign 3 for each edge, we can determine a sphairahedron. Other than that, after considering a Hamilton loop on the edge-graph of a regular dodecahedron, how about we assign 4, 4, 4, 4 or 3, 6, 3, 6 on the Hamilton loop and assign 2 on other edges. This way determines other sphairahedra.

Next is a regular octahedron. The degree of each vertex is 4; thus, we can assign 2 for every edge. The last example is a trivalent polyhedron. If we assign 3 for each edge, we can determine a sphairahedron. The simplest one is a truncated tetrahedron with 8 faces.

In general, it seems difficult for us to list up all sphairahedron with seven or more faces. About heptahedron, there are 34 kinds of polyhedral structures of convex hept-

tahedra. Furthermore, most of them are candidates to generate a sphairahedron. The number of polyhedra with eight or more faces explosively increases. See also [Michon 2020].

4. Observation

4.1. Visualization

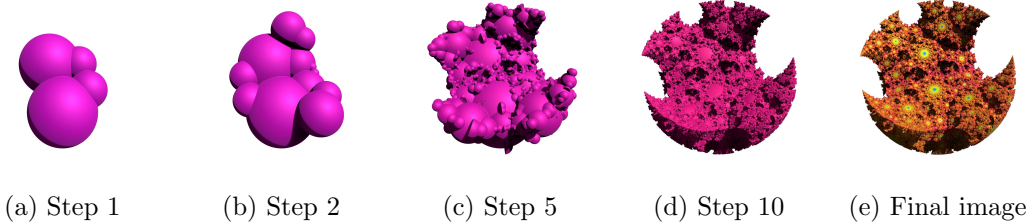


Figure 65.: Tiling of a finite cubic sphairahedron.

In section 2.2, we show how to construct the tiling patterns of sphairahedra and their coloring. After we compute the coordinates of a sphairahedron, we have to render an infinite number of sphairahedra, and it takes much time. So, we use an algorithm to render fractals based on inversions. It is called Iterated Inversion System (IIS.) We successfully implement a fast rendering algorithm combining IIS and sphere tracing, a kind of ray-tracing technique. For more details, see also [Nakamura et al. 2017] and [Nakamura et al. 2018].

There are two approaches to visualization. First, we tile the sphairahedra directly in the space using elements of the tiling group G . Secondly, we prepare some balls that include a sphairahedron, and we transform the spheres by G . We call the boundary of each ball a *ghost sphere*. See Figure 65. Four balls are preset, and we transform them by elements of G , and finally, we get the same quasi-sphere as the one in an original way. We can obtain a quasi-sphere from applying G to the union of the balls. We show the proof below.

For each vertex of the sphairahedron, we consider *maximum vertex ball* defined as followings.

Definition 4.1. Let T be an ideal sphairahedron and let X be one of the vertexes on T . An open ball B_X is a *maximum vertex ball* of X when the following conditions are satisfied.

- a) The boundary sphere ∂B_X of B_X passes through the vertex X , and ∂B_X is perpendicular to all of the edges gathering at X . (Remark that the edges are mutually tangent at X .)
- b) $B_X \cap T \neq \emptyset$ and B_X doesn't contain any vertex of T
- c) B_X is a maximal open ball satisfying a) and b) with respect to inclusions.

Remark 2. (1) The maximum vertex ball is well-defined for each vertex of a sphairahedron T .

(2) When the vertex X is the infinite-point, the maximum vertex ball is a half-space B_X satisfying followings:

- a) The boundary plane ∂B_X is perpendicular to the prism(, neighborhood of ∞ .)

The conditions b) and c) are the same as above.

Proposition 4.2. *Let T be a rational ideal sphairahedron and let $L = (T, G)$ be its tiling. The total tiling space $\cup_k |L|_k$ includes the maximum vertex ball B_X for any vertex X .*

Proof. Maximum vertex ball is *equivariant* for any Möbius transformations φ in S^3 . That is, if B_X is the maximum vertex ball of T at X , then $\varphi(B_X)$ is the maximum vertex ball of $\varphi(T)$ at $\varphi(X)$. Because the conditions a), b), and c) are preserved under the transformation φ .

Thus we may assume the following conditions for T and X .

- (i) The vertex X is the infinite-point ∞ .
- (ii) A neighborhood of $X = \infty$ is an infinite prism, parallel and elongated to the negative direction of the z -axis.

We can give $B_X = \{(x, y, z) \mid z < z_{\min}\}$ when

$$z_{\min} := \min\{z \mid (x, y, z) \text{ is a vertex of } T\}.$$

$B_X \cap T$ is a right prism infinitely parallel and elongated to the negative direction of the z -axis. The rationality condition of T guarantees that the tiling space of $B_X \cap T$ by face symmetry is B_X itself. Thus

$$B_X = \text{The tiling space of } B_X \cap T \subset \bigcup_k |L|_k$$

This completes the proof. \square

Theorem 4.3. *If $\bigcup_X B_X \supset T$, then*

$$\text{Cl} \left(\bigcup_{g \in G} g \left(\bigcup_X B_X \right) \right) = \text{Cl} \left(\bigcup_k |L|_k \right).$$

Here \bigcup_X means the union for some vertices X of T .

Proof. From the assumption $\bigcup_X B_X \supset T$,

$$\text{Cl} \left(\bigcup_{g \in G} g \left(\bigcup_X B_X \right) \right) \supset \text{Cl} \left(\bigcup_k |L|_k \right). \quad (4.A)$$

Conversely, from proposition 4.2, $\bigcup_X B_X \subset \bigcup_k |L|_k$ and we have

$$\bigcup_{g \in G} g \left(\bigcup_X B_X \right) \subset \bigcup_k |L|_k. \quad (4.B)$$

From (4.A) and (4.B), we have the conclusion. \square

4.2. Extended Schottky group for a cubic sphairahedron

Let $\varphi_i \in \text{M\"ob}(S^3)$ be the inversion of the face O_i . Let the tiling group G be a group generated by φ_i 's. From the rationality condition, we have relations

$$(\varphi_i \varphi_j)^{n_{ij}} = \text{id}$$

for (i, j) such that $e_{ij} := O_i \cap O_j \neq \emptyset$ is an edge and $\frac{\pi}{n_{ij}}$ is the dihedral angle at e_{ij} . Otherwise, there is no relation between φ_i and φ_j . Thus, we have that

$$G = \langle \varphi_1, \dots, \varphi_6 \mid (\varphi_i \varphi_j)^{n_{ij}} = \text{id} \text{ for } e_{ij} \text{ is an edge.} \rangle$$

The lengths of all relations are even numbers, and we can consider the subgroup G_+ consisting of all elements of even length. G_+ is an orientation preserving Möbius transformation group and $\Lambda(G) = \Lambda(G_+)$.

When a sphairahedron T is a cube of type 1, we can consider another transformation group representing the tiling of T . This proposition is written in the unpublished preprint [Ahara and Araki 2004], and we review the proof in this paper.

Proposition 4.4. *Let T be a cube of type 1 in Figure 37. Then there exist three (orientation preserving) Möbius transformations f_1, f_2, f_3 such that*

- (1) f_1 maps the inside of O_1 onto the outside of O_6 , $f_1(P_{135}) = P_{356}$, $f_1(P_{123}) = P_{236}F$, $f_1(P_{124}) = P_{246}$, and $f_1(P_{145}) = P_{456}$.
- (2) f_2 maps the inside of O_3 onto the outside of O_4 , $f_2(P_{135}) = P_{145}$, $f_2(P_{356}) = P_{456}$, $f_2(P_{236}) = P_{246}$, and $f_2(P_{123}) = P_{124}$.
- (3) f_2 maps the inside of O_2 onto the outside of O_5 , $f_2(P_{123}) = P_{135}$, $f_2(P_{236}) = P_{356}$, $f_2(P_{246}) = P_{456}$, and $f_2(P_{124}) = P_{145}$.

Let H be a subgroup of the orientation preserving Möbius transformation group $\text{M\"ob}_+(S^3)$, generated by f_1, f_2, f_3 . It follows that

$$H = \langle f_1, f_2, f_3 \mid (f_1 f_2)^3 = (f_2 f_3)^3 = (f_1 f_3)^3 = \text{id} \rangle$$

from this Proposition. It is easy to show that the fundamental domain of H is T and H generate the same tiling as that of G . Therefore $\Lambda(G) = \Lambda(H)$.

Proof. See Figure 36 and Figure 38(c). We redisplay Figure 38(c) as seen in Figure 66. This figure shows that all of the vertices of a cube lie on a plane. After elementary

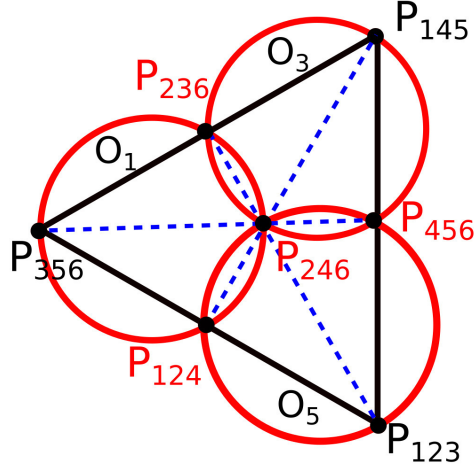


Figure 66.: All of the vertices of a cube lie on a plane.

calculations, we have the coordinates of the vertices as follows.

$$\begin{aligned}
 &P_{123} \left(\frac{1}{2}, -\frac{\sqrt{3}}{2}, 0 \right) \\
 &P_{145} \left(\frac{1}{2}, \frac{\sqrt{3}}{2}, z_4, \right) \\
 &P_{356} (-1, 0, z_6) \\
 &P_{124} \left(\frac{1}{2}, \frac{\sqrt{3}(r_2 - r_4)}{2(r_2 + r_4)}, \frac{r_2 z_4}{r_2 + r_4} \right) \\
 &P_{456} \left(\frac{r_6 - 2r_4}{2(r_4 + r_6)}, \frac{\sqrt{3}r_6}{2(r_4 + r_6)}, \frac{z_4 r_6 + z_6 r_4}{r_4 + r_6} \right) \\
 &P_{236} \left(\frac{r_6 - 2r_2}{2(r_2 + r_6)}, \frac{-\sqrt{3}r_6}{2(r_2 + r_6)}, \frac{r_2 z_6}{r_2 + r_6} \right)
 \end{aligned}$$

Let R be the intersection of the segment $P_{123}P_{456}$ and $P_{145}P_{236}$. (Indeed, three segments $P_{123}P_{456}$, $P_{145}P_{236}$, and $P_{356}P_{124}$ are concurrent.) The coordinate of R is

$$R \left(\frac{-2r_2 r_4 + r_2 r_6 + r_4 r_6}{2R}, \frac{\sqrt{3}(r_2 r_6 - r_4 r_6)}{2R}, \frac{r_2(r_6 z_4 + r_4 z_6)}{R} \right),$$

where $R = r_2 r_4 + r_4 r_6 + r_6 r_2$. The coordinate of the center C_2 of O_2 is given by

$C_2 \left(\frac{1-r_2}{2}, \frac{-\sqrt{3}(1-r_2)}{2}, 0 \right)$, then we have

$$\begin{aligned} C_2 R^2 &= \left(\frac{1-r_2}{2} - \frac{-2r_2 r_4 + r_2 r_6 + r_4 r_6}{2R} \right)^2 \\ &\quad + \left(\frac{-\sqrt{3}(1-r_2)}{2} - \frac{\sqrt{3}(r_2 r_6 - r_4 r_6)}{2R} \right)^2 \\ &\quad + \left(\frac{r_2(r_6 z_4 + r_4 z_6)}{R} \right)^2 \\ &= r_2^2 \end{aligned}$$

Remark that in this calculation we use relations $z_4^2 = 3(r_2 + r_4 - 1)$, $z_6^2 = 3(r_2 + r_6 - 1)$, and $2z_4 z_6 = 6r_2 - 3$. It follows that R is on the sphere O_2 . In the same way, we show that R is on O_4 and on O_6 . Therefore we obtain the result $R = P_{246}$

On the other hand, the three power of a point P_{356} are identified. That is,

$$P_{356}P_{236} \cdot P_{356}P_{123} = P_{356}P_{246} \cdot P_{356}P_{124} = P_{356}P_{456} \cdot P_{356}P_{145}$$

holds. Thus, let O_{356} a sphere with the center P_{356} and with radius $\sqrt{P_{356}P_{236} \cdot P_{356}P_{123}}$, and let φ_{356} be the inversion of O_{356} . Then

$$\varphi_{356}(P_{123}) = P_{236}, \varphi_{356}(P_{124}) = P_{246}, \varphi_{356}(P_{145}) = P_{456}, \varphi_{356}(\infty) = P_{356}$$

and the composite $\varphi_{356} \circ \varphi_1$ satisfies the conditions of f_1 . For f_2 and f_3 , we can find them in the similar way. \square

4.3. Patterns of Planes

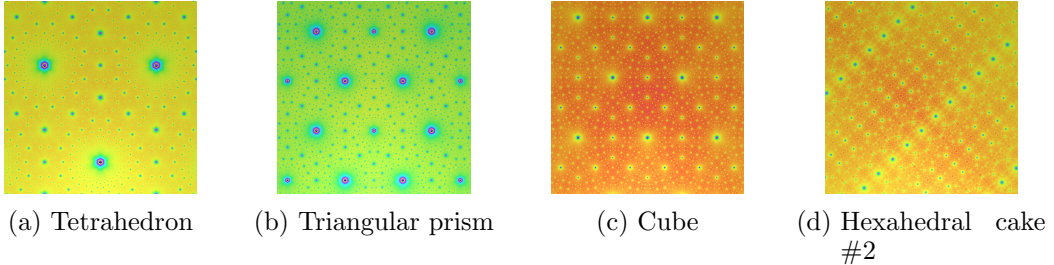


Figure 67.: Planes.

A cubic sphairahedron of type 1 is controlled by two parameters z_A and z_B . When both of the parameters equal to zero, the limit set is a plane (or a round sphere,) with a regular pattern as seen in Figure 67(c). Simillar patterns appear in other sphairahedra. See Figures 67 (a)(b) (c)(d). The patterns in (c) (a)(b) seems same as the cubes' pattern at all. We analyze these patterns.

First we consider the pattern in a tetrahedron. (See Section 3.2) The parameter space of a tetrahedron consists on one point. We use notations as in Section 3.2. Let $O_i = \partial \overline{D}_i$ be the boundary of balls and $C_i = O_i \cap (xy\text{-plane})$ be the section by the

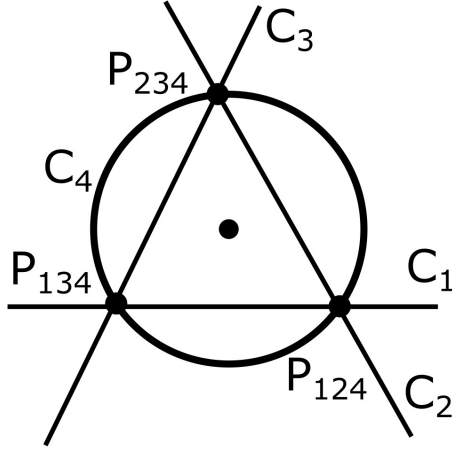


Figure 68.: C_i 's of tetrahedron.

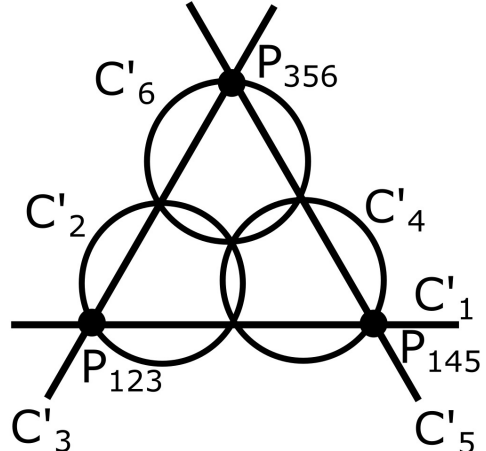


Figure 69.: C''_i 's of cube.

xy -plane. Three lines C_1 , C_2 , and C_3 establish a regular triangle. A circle C_4 is the circumscribed circle of the triangle. See Figure 68.

We embed C_i 's into the complex plane \mathbb{C} as follows.

$$P_{134}(0), \quad P_{123}(3), \quad P_{234}(3\omega),$$

where $\omega = \frac{1 + \sqrt{-3}}{2}$. The center of C_4 is $1 + \omega$.

If we let φ_i be the inversion of C_i , we can represent them by

$$\begin{aligned}\varphi_1(z) &= \bar{z} \\ \varphi_2(z) &= (-1 + \omega)\bar{z} \\ \varphi_3(z) &= -\omega\bar{z} + 3 + 3\omega \\ \varphi_4(z) &= \frac{(1 + \omega)\bar{z}}{\bar{z} - 2 + \omega}.\end{aligned}$$

Thus every coefficient is contained in the Eisenstein ring $\mathbb{Z}[\omega]$.

In case of cube of type1, we may have similar observations. In Figure 69 is the section of O_i 's in Section 3.4.3. Let $D_i = O_i \cap (xy\text{-plane})$ and ψ_i is the inversion of D_i . We embed D_i 's into \mathbb{C} by

$$P_{123}(0), \quad P_{145}(6), \quad P_{356}(6\omega).$$

Thus we have the following formulas:

$$\begin{aligned}
\psi_1(z) &= \bar{z} = \varphi_1(z) \\
\psi_2(z) &= \frac{(1+\omega)\bar{z}}{\bar{z}-2+\omega} = \varphi_4(z) \\
\psi_3(z) &= (-1+\omega)\bar{z} = \varphi_2(z) \\
\psi_4(z) &= \frac{(1+4\omega)\bar{z}-18}{\bar{z}-5+4\omega} = \varphi_1(z) = \varphi_2 \circ \varphi_1 \circ \varphi_4 \circ \varphi_1 \circ \varphi_2(z). \\
\psi_5(z) &= -\omega\bar{z}+6+6\omega = \varphi_2 \circ \varphi_1 \circ \varphi_3 \circ \varphi_1 \circ \varphi_2(z) \\
\psi_6(z) &= \frac{(4+\omega)\bar{z}-18}{\bar{z}-5+\omega} = \varphi_2 \circ \varphi_3 \circ \varphi_4 \circ \varphi_3 \circ \varphi_2(z).
\end{aligned}$$

These data inspire us a certain relationship between sphairahedra and bianchi tessellations of the Eisenstein ring, but this problem is fully open.

4.4. Outside of the parameter space

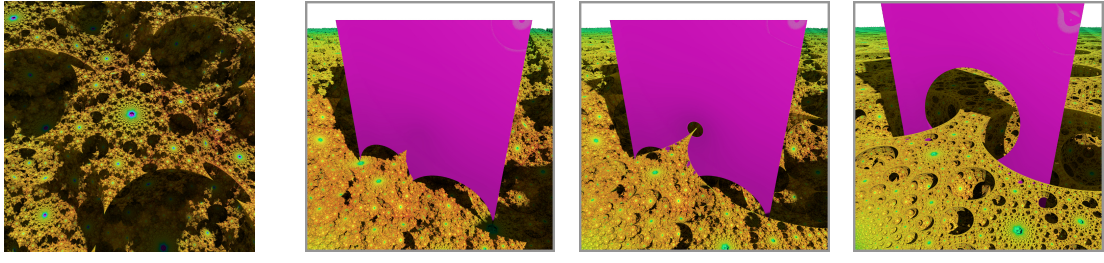


Figure 70.: Cube limit set
with arms.

Figure 71.: Cube limit set and upper part of sphairahedral prism.

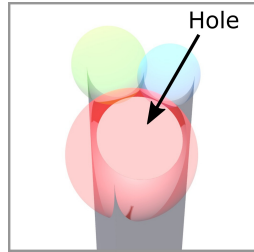


Figure 72.: Sphairahedron with hole.

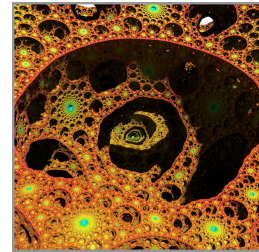


Figure 73.: Limit set with hole.

In this subsection we observe cubic infinite sphairahedron whose dihedral angles are $\pi/3$ and its parameter space. The parameter space is shown in Figure 40. The gray region of this figure shows the parameter space for ideal rational cubes. Figure 70 shows the limit set for the parameter pair (z_A, z_B) is very near $\left(\frac{\sqrt{6}}{4}, \frac{\sqrt{6}}{2}\right)$. Observing the shape of the limit set, we can find a cone-shaped arm (an elongated part, or a half of an arch bridge.) In the center of Figure 70, there is a hexagonal table-like shape, and there is an arm at each vertex. On the other hand, we can find another arm

from another hexagonal table-like shape, and two arms construct an unfinished arch bridge. We scrutinize this part. See Figures 71 (a)(b)(c). The pink block in each figure is ‘another connected component’ of the compliment $A = S^3 - \cup_i \overline{D_i}$. Theoretically saying, the pink block does not have an intersection with the limit set. Figure (a) shows an image where the parameter is very near the boundary of the parameter space. A tip of the arm is near the pink block, and at the same time, the block is skinny (like a tissue) around here.. Figure (b) shows an image where the parameter is a bit outside the parameter space. There occurs a small hole on the thin wall, and two arms are connecting (complete an arch bridge.) we call the arms *pinched arms*. Here, the compliment $A = S^3 - \cup_i \overline{D_i}$ has two connected components, and one of them is simply connected, but upper one is not, and this is not a sphairahedron. Figure (c) shows an image where the parameter is entirely outside the parameter space. The hole on the wall gets broader than that of (b), and the arch bridge gets stout. We call the arms *bridged arms*.

From the series of phenomena on arms, we may have a conjecture the existence of some particular elements in the tiling group G . One is the existence of an accidental parabolic element in G when the parameter lies on the boundary of the parameter space. The other is the existence of an elliptic element in G when the parameter lies outside the parameter space. Here we say that an element is parabolic (resp. elliptic) as a Möbius transformation.

Figure 72 shows another example of a ‘sphairahedron with a hole.’ In this case, there is a wall-hole in the lower component and the limit set has many tunnels shown in Figure 73.

5. Appendix - data

5.1. Cube

Type 1:

$$\begin{aligned}\overline{D_1} &= \{(x, y, z) \mid \frac{1}{2} \leq x\} \cup \{\infty\} \\ \overline{D_3} &= \{(x, y, z) \mid \frac{1}{2} \leq -\frac{1}{2}x - \frac{\sqrt{3}}{2}y\} \cup \{\infty\} \\ \overline{D_5} &= \{(x, y, z) \mid \frac{1}{2} \leq -\frac{1}{2}x + \frac{\sqrt{3}}{2}y\} \cup \{\infty\} \\ \overline{D_2} &= \{(x, y, z) \mid (x - x_2)^2 + (y - y_2)^2 + z^2 \leq r_2^2\} \\ \overline{D_4} &= \{(x, y, z) \mid (x - x_4)^2 + (y - y_4)^2 + (z - z_A)^2 \leq r_4^2\} \\ \overline{D_6} &= \{(x, y, z) \mid (x - x_6)^2 + (y - y_6)^2 + (z - z_B)^2 \leq r_6^2\} \\ r_2 &= \frac{2z_A z_B + 3}{6}, \quad (x_2, y_2) = \left(\frac{1}{2}(1 - r_2), -\frac{\sqrt{3}}{2}(1 - r_2) \right), \\ r_4 &= \frac{2z_A(z_A - z_B) + 3}{6}, \quad (x_4, y_4) = \left(\frac{1}{2}(1 - r_4), \frac{\sqrt{3}}{2}(1 - r_4) \right), \\ r_6 &= \frac{2z_B(z_B - z_A) + 3}{6}, \quad (x_6, y_6) = (r_6 - 1, 0),\end{aligned}$$

The parameter space is as follows.

The parameter space is shown in Figure40.

$$\begin{aligned}
 (1) z_A z_B &= 3/4 \\
 (2) z_B^2 - z_A z_B &= 3/4 \\
 (3) z_A^2 - z_A z_B &= 3/4
 \end{aligned}$$

Type 2:

$$\begin{aligned}
 \overline{D_1} &= \{(x, y, z) \mid y \geq -\frac{\sqrt{3}}{3}x + \frac{\sqrt{3}}{3}\} \cup \{\infty\} \\
 \overline{D_3} &= \{(x, y, z) \mid y \geq \frac{\sqrt{3}}{3}x - \frac{\sqrt{3}}{3}\} \cup \{\infty\} \\
 \overline{D_5} &= \{(x, y, z) \mid x \leq -0.5\} \cup \{\infty\} \\
 \overline{D_2} &= \{(x, y, z) \mid (x - x_2)^2 + (y - y_2)^2 + z^2 \leq r_2^2\} \\
 \overline{D_4} &= \{(x, y, z) \mid (x - x_4)^2 + (y - y_4)^2 + (z - z_A)^2 \leq r_4^2\} \\
 \overline{D_6} &= \{(x, y, z) \mid (x - x_6)^2 + (y - y_6)^2 + (z - z_B)^2 \leq r_6^2\} \\
 r_2 &= \frac{2\sqrt{3}z_A z_B 3\sqrt{3}}{9}, \quad (x_2, y_2) = \left(1 - r_2 \frac{\sqrt{3}}{2}, \frac{r_2}{2}\right), \\
 r_4 &= \frac{3z_A^2 - 4z_A z_B + 3}{9}, \quad (x_4, y_4) = \left(-\frac{1 - r_4}{2}, \frac{(1 - r_4)\sqrt{3}}{2}\right), \\
 r_6 &= \frac{3z_B^2 - 2z_A z_B + 6}{9}, \quad (x_6, y_6) = \left(-\frac{1 - r_6}{2}, -\frac{(1 - r_6)\sqrt{3}}{2}\right),
 \end{aligned}$$

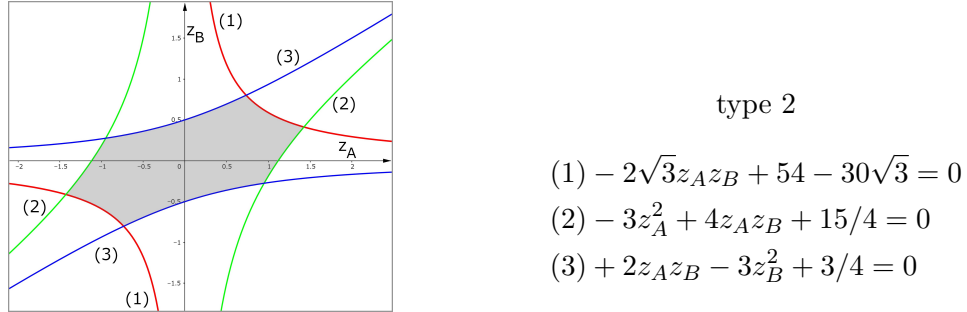


Figure 74.: Parameter space of type 2.

Type 3:

$$\overline{D_1} = \{(x, y, z) \mid y \geq -\frac{\sqrt{3}}{3}x + \frac{\sqrt{3}}{3}\} \cup \{\infty\}$$

$$\overline{D_3} = \{(x, y, z) \mid y \leq \frac{\sqrt{3}}{3}x - \frac{\sqrt{3}}{3}\} \cup \{\infty\}$$

$$\overline{D_5} = \{(x, y, z) \mid x \leq -0.5\} \cup \{\infty\}$$

$$\overline{D_2} = \{(x, y, z) \mid (x - x_2)^2 + (y - y_2)^2 + z^2 \leq r_2^2\}$$

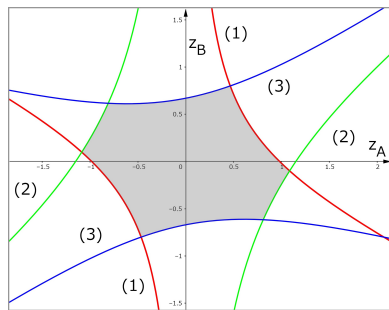
$$\overline{D_4} = \{(x, y, z) \mid (x - x_4)^2 + (y - y_4)^2 + (z - z_A)^2 \leq r_4^2\}$$

$$\overline{D_6} = \{(x, y, z) \mid (x - x_6)^2 + (y - y_6)^2 + (z - z_B)^2 \leq r_6^2\}$$

$$r_2 = \frac{z_A^2 + 2z_A z_B + 6}{5\sqrt{3}}, \quad (x_2, y_2) = \left(1 - \frac{r_2\sqrt{3}}{2}, \frac{r_2}{2}\right),$$

$$r_4 = \frac{3z_A^2 - 4z_A z_B + 3}{5\sqrt{3}}, \quad (x_4, y_4) = \left(-0.5, \frac{\sqrt{3}}{2} - r_4\right),$$

$$r_6 = \frac{-z_A^2 - 2z_A z_B + 5z_B^2 + 9}{15}, \quad (x_6, y_6) = \left(-\frac{1 - r_6}{2}, -\frac{\sqrt{3}(1 - r_4)}{2}\right),$$



type 3

$$(1) - \sqrt{3}z_A^2 - 2\sqrt{3}z_A z_B + 90 - 51\sqrt{3} = 0$$

$$(2) - 3\sqrt{3}z_A^2 + 4\sqrt{3}z_A z_B + 90 - 48\sqrt{3} = 0$$

$$(3) z_A^2 + 2z_A z_B - 5z_B^2 + 9/4 = 0$$

Figure 75.: Parameter space of type 3.

Type 4:

$$\overline{D_1} = \{(x, y, z) \mid y \geq \sqrt{3}x\} \cup \{\infty\}$$

$$\overline{D_3} = \{(x, y, z) \mid y \geq -\sqrt{3}x + \sqrt{3}\} \cup \{\infty\}$$

$$\overline{D_5} = \{(x, y, z) \mid y \leq \frac{\sqrt{3}}{3}x - \frac{\sqrt{3}}{3}\} \cup \{\infty\}$$

$$\overline{D_2} = \{(x, y, z) \mid (x - x_2)^2 + (y - y_2)^2 + z^2 \leq r_2^2\}$$

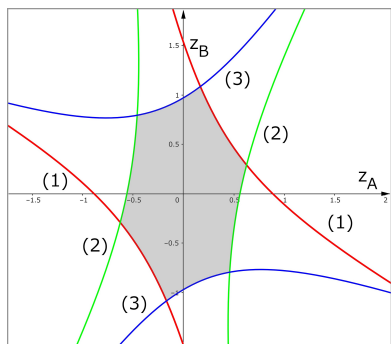
$$\overline{D_4} = \{(x, y, z) \mid (x - x_4)^2 + (y - y_4)^2 + (z - z_A)^2 \leq r_4^2\}$$

$$\overline{D_6} = \{(x, y, z) \mid (x - x_6)^2 + (y - y_6)^2 + (z - z_B)^2 \leq r_6^2\}$$

$$r_2 = \frac{3z_A^2 + z_B^2 + 6z_A z_B + 6}{18}, \quad (x_2, y_2) = (1 - r_2, 0),$$

$$r_4 = \frac{15z_A^2 - z_B^2 - 6z_A z_B + 12}{18\sqrt{3}}, \quad (x_4, y_4) = \left(0.5, \frac{\sqrt{3}}{2} - r_4\right),$$

$$r_6 = \frac{-3z_A^2 + 5z_B^2 - 6z_A z_B + 12}{18}, \quad (x_6, y_6) = \left(-\frac{1 - r_6}{2}, -\frac{\sqrt{3}(1 - r_6)}{2}\right),$$



type 4

$$(1) - 3z_A^2 - 6z_A z_B - z_B^2 - 60 + 36\sqrt{3} = 0$$

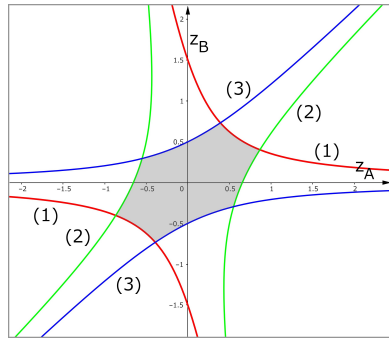
$$(2) - 15z_A^2 + 6z_A z_B + z_B^2 - 120 + 72\sqrt{3} = 0$$

$$(3) 3z_A^2 + 6z_A z_B - 5z_B^2 - 120 + 72\sqrt{3} = 0$$

Figure 76.: Parameter space of type 4.

Type 5:

$$\begin{aligned}
\overline{D_1} &= \{(x, y, z) \mid y \geq \sqrt{3}x\} \cup \{\infty\} \\
\overline{D_3} &= \{(x, y, z) \mid y \geq -\sqrt{3}x + \sqrt{3}\} \cup \{\infty\} \\
\overline{D_5} &= \{(x, y, z) \mid y \leq \frac{\sqrt{3}}{3}x - \frac{\sqrt{3}}{3}\} \cup \{\infty\} \\
\overline{D_2} &= \{(x, y, z) \mid (x - x_2)^2 + (y - y_2)^2 + z^2 \leq r_2^2\} \\
\overline{D_4} &= \{(x, y, z) \mid (x - x_4)^2 + (y - y_4)^2 + (z - z_A)^2 \leq r_4^2\} \\
\overline{D_6} &= \{(x, y, z) \mid (x - x_6)^2 + (y - y_6)^2 + (z - z_B)^2 \leq r_6^2\} \\
r_2 &= \frac{z_B^2 + 6z_A z_B + 3}{7\sqrt{3}}, \quad (x_2, y_2) = \left(1 - \frac{\sqrt{3}}{2}r_2, \frac{r_2}{2}\right), \\
r_4 &= \frac{7z_A^2 - z_B^2 - 6z_A z_B + 4}{14}, \quad (x_4, y_4) = \left(\frac{1+r_4}{2}, (1-r_4)\frac{\sqrt{3}}{2}\right), \\
r_6 &= \frac{2z_B^2 - 2z_A z_B + 6}{7}, \quad (x_6, y_6) = \left(-\frac{1-r_6}{2}, -\frac{\sqrt{3}}{2}(1-r_6)\right),
\end{aligned}$$



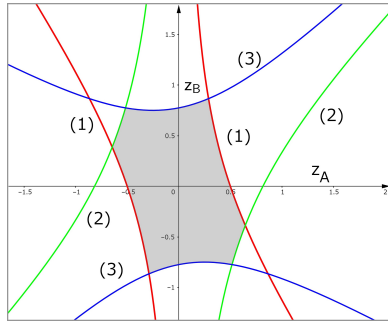
type 5

$$\begin{aligned}
(1) \quad &6z_A z_B - z_B^2 + 9/4 = 0 \\
(2) \quad &7z_A^2 - 6z_A z_B - z_B^2 - 3 = 0 \\
(3) \quad &z_A z_B - z_B^2 - 24 + 14\sqrt{3} = 0
\end{aligned}$$

Figure 77.: Parameter space of type 5.

Type 8:

$$\begin{aligned}
\overline{D_1} &= \{(x, y, z) \mid y \geq \sqrt{3}x\} \cup \{\infty\} \\
\overline{D_3} &= \{(x, y, z) \mid y \geq -\sqrt{3}x + \sqrt{3}\} \cup \{\infty\} \\
\overline{D_5} &= \{(x, y, z) \mid y \leq \frac{\sqrt{3}}{3}x - \frac{\sqrt{3}}{3}\} \cup \{\infty\} \\
\overline{D_2} &= \{(x, y, z) \mid (x - x_2)^2 + (y - y_2)^2 + z^2 \leq r_2^2\} \\
\overline{D_4} &= \{(x, y, z) \mid (x - x_4)^2 + (y - y_4)^2 + (z - z_A)^2 \leq r_4^2\} \\
\overline{D_6} &= \{(x, y, z) \mid (x - x_6)^2 + (y - y_6)^2 + (z - z_B)^2 \leq r_6^2\} \\
r_2 &= \frac{3z_A^2 + 2z_A z_B + 3}{5\sqrt{3}}, \quad (x_2, y_2) = \left(1 - \frac{\sqrt{3}}{2}r_2, \frac{r_2}{2}\right), \\
r_4 &= \frac{2(z_A^2 - z_A z_B + 1)}{5}, \quad (x_4, y_4) = \left(\frac{1 - r_4}{2}, \frac{\sqrt{3}(1 - r_4)}{2}\right), \\
r_6 &= \frac{-3z_A^2 - 2z_A z_B + 5z_B^2 + 12}{10\sqrt{3}}, \quad (x_6, y_6) = \left(\frac{\sqrt{3}r_6 - 1}{2}, \frac{-\sqrt{3} + r_6}{2}\right),
\end{aligned}$$



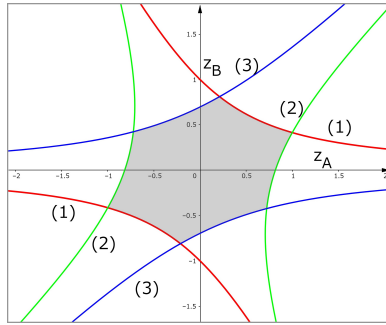
type 8

$$\begin{aligned}
(1) \quad &3z_A^2 - 2z_A z_B + 3/4 = 0 \\
(2) \quad &3z_A^2 + 3z_A z_B + 2 = 0 \\
(3) \quad &3z_A^2 + 2z_A z_B - 5z_B^2 + 3 = 0
\end{aligned}$$

Figure 78.: Parameter space of type 8.

Type 9:

$$\begin{aligned}
\overline{D_1} &= \{(x, y, z) \mid x \leq 0\} \cup \{\infty\} \\
\overline{D_3} &= \{(x, y, z) \mid y \geq -x + 1\} \cup \{\infty\} \\
\overline{D_5} &= \{(x, y, z) \mid y \leq x - 1\} \cup \{\infty\} \\
\overline{D_2} &= \{(x, y, z) \mid (x - x_2)^2 + (y - y_2)^2 + z^2 \leq r_2^2\} \\
\overline{D_4} &= \{(x, y, z) \mid (x - x_4)^2 + (y - y_4)^2 + (z - z_A)^2 \leq r_4^2\} \\
\overline{D_6} &= \{(x, y, z) \mid (x - x_6)^2 + (y - y_6)^2 + (z - z_B)^2 \leq r_6^2\} \\
r_2 &= \frac{z_B^2 + 2z_A z_B + 2}{6}, \quad (x_2, y_2) = (1 - r_2, 0), \\
r_4 &= \frac{\sqrt{2}(3z_A^2 - 2z_A z_B - z_B^2 + 4)}{12}, \quad (x_4, y_4) = \left(\frac{r_4}{\sqrt{2}}, 1 - \frac{r_4}{\sqrt{2}}\right), \\
r_6 &= \frac{z_B^2 - z_A z_B + 2}{3}, \quad (x_6, y_6) = (0, r_6 - 1),
\end{aligned}$$



type 9

$$\begin{aligned}
 (1) - 2z_A z_B - z_B^2 + 1 &= 0 \\
 (2) - 3z_A^2 + 2z_A z_B + z_B^2 + 2 &= 0 \\
 (3) z_A z_B - z_B^2 - 8 + 6\sqrt{2} &= 0
 \end{aligned}$$

Figure 79.: Parameter space of type 9.

5.2. Cake #2

Type 1:

$$\overline{D_1} = \{(x, y, z) \mid y \geq -x + 1\} \cup \{\infty\}$$

$$\overline{D_2} = \{(x, y, z) \mid y \geq x + 1\} \cup \{\infty\}$$

$$\overline{D_3} = \{(x, y, z) \mid y \leq -x + 1 - \frac{(2+z_A^2)\sqrt{3}}{4}\} \cup \{\infty\}$$

$$\overline{D_4} = \{(x, y, z) \mid y \leq x - 1\} \cup \{\infty\}$$

$$\overline{D_5} = \{(x, y, z) \mid (x - x_5)^2 + (y - y_5)^2 + z^5 \leq r_5^2\}$$

$$\overline{D_6} = \{(x, y, z) \mid (x - x_6)^2 + (y - y_6)^2 + (z - z_A)^2 \leq r_6^2\}$$

$$r_5 = \frac{2+z_A^2}{4\sqrt{2}}, \quad (x_5, y_5) = \left(-\frac{r_5(\sqrt{6}-\sqrt{2})}{4}, 1 - \frac{r_5(\sqrt{6}+\sqrt{2})}{4} \right),$$

$$r_6 = \frac{(2+z_A^2)\sqrt{6}}{8}, \quad (x_6, y_6) = \left(1 - \frac{r_6}{\sqrt{2}} - \frac{r_6(\sqrt{6}-\sqrt{2})}{4}, -\frac{r_6}{\sqrt{2}} + \frac{r_6(\sqrt{6}+\sqrt{2})}{4} \right),$$

The parameter space is $-\sqrt{\frac{10-4\sqrt{3}}{3+2\sqrt{3}}} < z_A < \sqrt{\frac{10-4\sqrt{3}}{3+2\sqrt{3}}}.$

Type 2:

$$\begin{aligned}
\overline{D_1} &= \{(x, y, z) \mid y \geq -x + 1\} \cup \{\infty\} \\
\overline{D_2} &= \{(x, y, z) \mid y \geq x + 1\} \cup \{\infty\} \\
\overline{D_3} &= \{(x, y, z) \mid y \leq -x + 1 - \frac{2+z_A^2}{2}\} \cup \{\infty\} \\
\overline{D_4} &= \{(x, y, z) \mid y \leq x - 1\} \cup \{\infty\} \\
\overline{D_5} &= \{(x, y, z) \mid (x - x_5)^2 + (y - y_5)^2 + z^5 \leq r_5^2\} \\
\overline{D_6} &= \{(x, y, z) \mid (x - x_6)^2 + (y - y_6)^2 + (z - z_A)^2 \leq r_6^2\} \\
r_5 &= \frac{2+z_A^2}{4}, \quad (x_5, y_5) = \left(0, 1 - \frac{2+z_A^2}{4}\right), \\
r_6 &= \frac{2+z_A^2}{4}, \quad (x_6, y_6) = \left(1 - \frac{2+z_A^2}{4}, 0\right),
\end{aligned}$$

The parameter space is $-\sqrt{8\sqrt{2}-10} < z_A < \sqrt{8\sqrt{2}-10}$.

Type 3:

$$\begin{aligned}
\overline{D_1} &= \{(x, y, z) \mid y \geq -x + 1\} \cup \{\infty\} \\
\overline{D_2} &= \{(x, y, z) \mid y \geq x + 1\} \cup \{\infty\} \\
\overline{D_3} &= \{(x, y, z) \mid y \leq -x + 1 - \frac{2+z_A^2}{2\sqrt{3}}\} \cup \{\infty\} \\
\overline{D_4} &= \{(x, y, z) \mid y \leq x - 1\} \cup \{\infty\} \\
\overline{D_5} &= \{(x, y, z) \mid (x - x_5)^2 + (y - y_5)^2 + z^5 \leq r_5^2\} \\
\overline{D_6} &= \{(x, y, z) \mid (x - x_6)^2 + (y - y_6)^2 + (z - z_A)^2 \leq r_6^2\} \\
r_5 &= \frac{2+z_A^2}{2\sqrt{6}}, \quad (x_5, y_5) = \left(r_5 \frac{\sqrt{6}-\sqrt{2}}{4}, 1 - r_5 \frac{\sqrt{6}+\sqrt{2}}{4}\right), \\
r_6 &= \frac{2+z_A^2}{2\sqrt{6}}, \quad (x_6, y_6) = \left(1 - \frac{r_5}{\sqrt{2}} - r_6 \frac{\sqrt{6}-\sqrt{2}}{4}, -\frac{r_5}{\sqrt{2}} + r_6 \frac{\sqrt{6}+\sqrt{2}}{4}\right),
\end{aligned}$$

The parameter space is $-\sqrt{2(8\sqrt{3}-13)} < z_A < \sqrt{2(8\sqrt{3}-13)}$.

5.3. Cake #3

Type 1:

$$\begin{aligned}
\overline{D_1} &= \{(x, y, z) \mid y \geq -x + 1\} \cup \{\infty\} \\
\overline{D_2} &= \{(x, y, z) \mid y \geq x + 1\} \cup \{\infty\} \\
\overline{D_3} &= \{(x, y, z) \mid y \leq -x + 1 - \frac{2}{\sqrt{3}}\} \cup \{\infty\} \\
\overline{D_4} &= \{(x, y, z) \mid y \leq x - 1\} \cup \{\infty\} \\
\overline{D_5} &= \{(x, y, z) \mid (x - x_5)^2 + (y - y_5)^2 + z^5 \leq r_5^2\} \\
\overline{D_6} &= \{(x, y, z) \mid (x - x_6)^2 + (y - y_6)^2 + (z - z_A)^2 \leq r_6^2\} \\
r_5 &= \frac{\sqrt{6}}{3}, \quad (x_5, y_5) = \left(1 - \frac{r_5}{4}(\sqrt{6} + \sqrt{2}), \frac{r_5}{4}(\sqrt{6} - \sqrt{2})\right), \\
r_6 &= \frac{z_A^2}{\sqrt{2}}, \quad (x_6, y_6) = \left(1 - \frac{1}{\sqrt{3}} + \frac{r_6}{4}(\sqrt{6} - \sqrt{2}), -\frac{1}{\sqrt{3}} + \frac{r_6}{4}(\sqrt{6} + \sqrt{2})\right),
\end{aligned}$$

The parameter space is $-\sqrt{\frac{-12+8\sqrt{3}}{3}} < z_A < \sqrt{\frac{-12+8\sqrt{3}}{3}}$.

Type 2:

$$\begin{aligned}
\overline{D_1} &= \{(x, y, z) \mid y \geq -x + 1\} \cup \{\infty\} \\
\overline{D_2} &= \{(x, y, z) \mid y \geq x + 1\} \cup \{\infty\} \\
\overline{D_3} &= \{(x, y, z) \mid y \leq -x - 1\} \cup \{\infty\} \\
\overline{D_4} &= \{(x, y, z) \mid y \leq x - 1\} \cup \{\infty\} \\
\overline{D_5} &= \{(x, y, z) \mid (x - x_5)^2 + (y - y_5)^2 + z^5 \leq r_5^2\} \\
\overline{D_6} &= \{(x, y, z) \mid (x - x_6)^2 + (y - y_6)^2 + (z - z_A)^2 \leq r_6^2\} \\
r_5 &= 1, \quad (x_5, y_5) = (0, 0), \\
r_6 &= \frac{z_A^2}{2}, \quad (x_6, y_6) = (-1 + r_6),
\end{aligned}$$

The parameter space is $-2\sqrt{\sqrt{2}-1} < z_A < 2\sqrt{\sqrt{2}-1}$.
(7441 words.)

References

- [Hart 1995] John C Hart, *Sphere Tracing: A Geometric Method for the Antialiased Ray Tracing of Implicit Surfaces* In: The Visual Computer 12, (1996), pp. 527–545
- [Mumford et. al. 2002] David Mumford, Caroline Series, and David Wright. *Indra's Pearls: The Vision of Felix Klein*, 1st ed. Apr. 2002.
- [Ahara and Araki 2003] Ahara, K. and Araki, Y., *Sphairahedral approach to parame-*

- terize visible three dimensional quasi-Fuchsian fractals*, Proceedings of Computer Graphics International, (2003), pp. 226–229.
- [Ahara 2003] Ahara, K., *Sphairahedra and three dimensional quasi-fuchsian group*, (in Japanese), RIMS Kokyuroku (Kyoto University), **1329**, (2003), pp.109-114
- [Ahara and Araki 2004] Ahara, K. and Araki, Y., *Classification of Ideal Regular Sphairahedra*, preprint, (2003).
- [Nakamura et al. 2016] Nakamura, K. and Kazushi Ahara, *A New Algorithm for Rendering Kissing Schottky Groups*, Proceedings of Bridges 2016: Mathematics, Music, Art, Architecture, Education, Culture, Tessellations Publishing, Phoenix, Arizona, (2016), pp. 367–370.
- [Kageyama 2016] Ryo Kageyama, *Configuration space and Limit set of sphaira-gons and sphaira-hedra*, (in Japanese), Master thesis in Nagoya University, 2016
- [Nakamura et al. 2017] Kento Nakamura and Kazushi Ahara, *A Geometrical Representation and Visualization of Möbius Transformation Groups*, Proceedings of Bridges 2017: Mathematics, Music, Art, Architecture, Education, Culture, Tessellations Publishing, Phoenix, Arizona, 2017, pp. 159–166.
- [Nakamura et al. 2018] Kento Nakamura and Kazushi Ahara, *Sphairahedra and Three-Dimensional Fractals*, Proceedings of Bridges 2018: Mathematics, Music, Art, Architecture, Education, Culture, Tessellations Publishing, Phoenix, Arizona, 2018, pp. 171–178.
- [Michon 2020] Gérard P. Michon, *Counting Polyhedra*,
<http://www.numericana.com/data/polyhedra.htm> (as of February 23 2020)
- [Nakamura 2020] Kento Nakamura, *sphairahedron.net*, <https://sphairahedron.net> (as of February 23 2020)